

## REVIEW

# Advanced two-dimensional materials toward polysulfides regulation of metal–sulfur batteries

Haining Fan<sup>1</sup> | Wenbin Luo<sup>2</sup> | Shixue Dou<sup>3</sup> | Zijian Zheng<sup>1,4,5,6</sup> 

<sup>1</sup>School of Fashion and Textiles, The Hong Kong Polytechnic University, Hong Kong, China

<sup>2</sup>Section of Environmental Protection Key Laboratory of Eco-Industry, Institute for Energy Electrochemistry and Urban Mines Metallurgy, School of Metallurgy, Northeastern University, Shenyang, China

<sup>3</sup>Institute of Energy Materials Science (IEMS), University of Shanghai for Science and Technology, Shanghai, China

<sup>4</sup>Department of Applied Biology and Chemical Technology, Faculty of Science, The Hong Kong Polytechnic University, Hong Kong, China

<sup>5</sup>Research Institute for Intelligent Wearable Systems, The Hong Kong Polytechnic University, Hong Kong, China

<sup>6</sup>Research Institute for Smart Energy, The Hong Kong Polytechnic University, Hong Kong, China

## Correspondence

Zijian Zheng, School of Fashion and Textiles, The Hong Kong Polytechnic University, Hong Kong, China.  
Email: [tczzheng@polyu.edu.hk](mailto:tczzheng@polyu.edu.hk)

## Funding information

Guangdong-Hong Kong-Macau Joint Laboratory for Photonic-Thermal-Electrical Energy Materials and Devices, Grant/Award Number: GDSTC No. 2019B121205001; Science and Technology Bureau of Huangpu District, Grant/Award Number: 2020GH03; Innovation and Technology Fund-Partnership Research Programme, Grant/Award Number: PRP/055/21FX; Innovation and Technology Fund-Guangdong Hong Kong Technology Cooperation Funding Scheme, Grant/Award Number: GHP/047/20GD

## Abstract

Metal–sulfur battery, which provides considerable high energy density at a low cost, is an appealing energy-storage technology for future long-range electric vehicles and large-scale power grids. One major challenge of metal–sulfur batteries is their long-term cycling stability, which is significantly deteriorated by the generation of various soluble polysulfide intermediates and the shuttling of these intermediates through the separator. Furthermore, the intrinsically sluggish reaction kinetics associated with the poor conductivity of sulfur/sulfides family causes a large polarization in cycle behavior, which further deteriorates the electrode rechargeability. To solve these problems, the research communities have spent a great amount of effort on designing smart cathodes to delicately tailor the physiochemical interaction between the sulfur hosts and polysulfides. Here, we summarize the key progress in the development of two-dimensional (2D) host materials showing advantageous tunability of their physiochemical properties through coordination control methods such as defect engineering, heteroatom doping, heterostructure, and phase and interface engineering. Accordingly, we discuss the mechanisms of polysulfide anchoring and catalyzing upon specific coordination environment in conjunction with possible structure–property relationships and theoretical analysis. This review will provide prospective fundamental guidance for future sulfur host design and beyond.

## KEYWORDS

2D materials, electrode engineering, energy storage, metal–sulfur batteries, polysulfide regulation

This is an open access article under the terms of the Creative Commons Attribution License, which permits use, distribution and reproduction in any medium, provided the original work is properly cited.

© 2023 The Authors. *SmartMat* published by Tianjin University and John Wiley & Sons Australia, Ltd.

## 1 | INTRODUCTION

Sulfur (S) cathode coupling with metallic anodes (such as Li, Na, K, etc.) presents great potential toward forthcoming electrification of transport, mainly due to the remarkable theoretical specific capacity of sulfur (1673 mA·h/g) and metal anodes (3860 mA·h/g of Li, 1166 mA·h/g of Na, 687 mA·h/g of K).<sup>1–8</sup> Calculated based on an average voltage of 2.15 V, Li-S battery can therefore deliver theoretical energy density of around 2500 W·h/kg on the assumption of complete reaction of Li with S to form Li<sub>2</sub>S, significantly greater than the practical lithium-ion battery (200 W·h/kg).<sup>4,9–12</sup> Yet, under real cycling conditions, cell performance falls substantially behind theoretical values. The responsible reason relies on an essential complex conversion reaction, which is heavily impacted by the specific physicochemical characteristics of all cell constituents. The insulating property of sulfur and sulfide species, the dissolution of polysulfides into electrolytes, the volumetric expansion at the cathode on cycling, and the creation of a dendritic anode are widely acknowledged as the primary causes of the undesirable performance. Particularly, in response to high-energy-density practical requirements, current studies refer to establishing high-loading cells of higher than 7 mg/cm<sup>2</sup> supported by reasonably lean electrolytes while still attaining high electrochemical utilization. In this situation, the aforementioned problems are amplified due to the difficulty in creating continuous electron/ion channels over a thick cathode.<sup>13–15</sup> Finally, despite the fact that Na/K-S cells have comparable chemistry with Li-S chemistry, there are some new issues that Na-S or K-S battery faces, such as poor ion transport and more sluggish conversion kinetics, caused by their larger ions and less reducing than Li ion.<sup>16–18</sup>

By far, in terms of tackling the aforementioned difficulties, extensive research has focused on exploring the original electrolyte through the tuning formula, salts as well as additives, and tailoring both metal anode and sulfur cathode.<sup>19–24</sup> Indeed, a promising durable performance is the result of comprehensive enhancement from all aspects in parallel, while sulfur cathode engineering is of key importance. Over past decades, impregnating sulfur into various carbonaceous materials as the conductive matrix is well developed to not only restrain polysulfides within the cathode but enhance their conversion reaction.<sup>25,26</sup> Early studies are focusing on altering inner pore or layer structure so as to better restrict polysulfides within the carbon skeleton, with typical examples such as diverse meso- and microporous carbon, carbon nanotube and fiber, graphene, and mixes thereof.<sup>27,28</sup> However, this simple spatial restriction is

insufficient, and only a few 100 cycles are obtained. Over this concept, it was discovered that doping heteroatoms (B, N, O, P, S, etc.) or introducing particular functional groups (–OH/–O–, –NH<sub>2</sub>, –SO<sub>3</sub>Ph, etc.) over carbon skeleton results in more efficient polar-to-polar interaction with sulfides species, which boosts cell capacity and cycling life to a certain extent.<sup>29,30</sup> Following this basis, a variety of materials embracing both metallic and nonmetallic compounds have been demonstrated as viable hosts for confining polysulfides via chemically enhanced interactions, such as polar–polar interaction and Lewis acid-base contact or sulfur-chain catenation.

Due to their distinctive 2D structure and tunable physicochemical property, 2D materials show significant advantages toward polysulfides regulation.<sup>31–33</sup> For instance, the large lateral size combined with controllable interspace greatly increases the loading area for sulfur as well as active sites exposed for suppressing “shuttling effect” and thereby stabilizing performance.<sup>34–36</sup> Graphitic carbon, the most typical 2D material, has been paid special attention, due to sufficient electron conductivity, which is quite important for high sulfur utilization in thick electrode cells.<sup>37–39</sup> Through the purposed functionalization by functional groups or hetero dopants, the such generated interface allows chemically enhanced polar-to-polar interaction with polysulfide intermediates via efficient charge transfer.<sup>29,40</sup> Apart from graphene, graphitic carbon nitride (g-C<sub>3</sub>N<sub>4</sub>), black phosphorus (BP), boron nitride (BN), and so forth, representing another type of 2D metal-free host materials, also gain burgeoning concerns. On it, the high concentration of electronegatively charged atoms in the lattice, along with asymmetric occupation, causes asymmetric charge distribution, affecting the net polarity and thus creating active sites for binding polysulfides.<sup>41,42</sup> Moreover, while this 2D layered structure brings about an enlarged lamellar area in the plane, the extremely sacrificed thickness associated with high surface energy results in severe aggregation, largely reducing the exposure area for polysulfides regulation. In practice to solve this problem, crosslinking robust 3D architecture from these 2D materials is adopted to date to increase the surface-to-volume ratio for high sulfur loading and therefore promote the energy and power density, which can be extended into metal or metal compounds as well.

Metals and metal compounds, typically including metal oxides/hydroxides/chalcogenides/nitrides/phosphides/borides/carbides as well as metal-organic frameworks, have been demonstrated as appealing nanomaterials to realize preferential adsorption and then redox reaction of polysulfides over than metal-free graphitic carbon or its analogs. Generally, metal centers

serving as Lewis acids are able to bind polysulfide anions while the paired anions such as oxide or chalcogen anions synergistically interact with the Li, Na, and K ions.<sup>43–46</sup> Particularly, some kinds of metals, such as Pt, Co, Ni, and so forth, could significantly facilitate conversion kinetics by modifying the reaction energy barrier, which thus narrows polarization potential difference and then maximizes energy utilization.<sup>47–50</sup> This anchoring and catalyzing effect derived from chemically-active Lewis acid-base pairs is largely influenced by specific coordination environment around central metal atoms. Considering this aspect, fine-tuning its composition via defect engineering, heteroatom doping, heterostructure construction, phase control, and their hybridization is applied to vary electronic distribution and hence enhance chemical interaction with polysulfides intermediates.<sup>51–55</sup> Unfortunately, compared with graphite carbon, the poor conductivity from metal/metal compounds makes it a tougher case for a fast redox reaction, and thus further hybridization with conductive additives is required, which however reduces its energy density.

By far, there has been growing research on the mechanism exploration of sulfur redox reaction as well as host material design; nevertheless, highly effective sulfur cathode with desirable cycling performance up to applicable criteria has yet to be developed. Fortunately, fast-growing high-quality characterization and in situ techniques have recently made significant progress in establishing a credible relationship between structural evolution and electrochemical performance on real-working status.<sup>56–58</sup> In this Review, we first give insights into the fundamental discharge-charge principle of the metal-sulfur battery together with inherent limitations toward application. And then, key progress made on robust cathodes design and corresponding effective interaction with polysulfides are systematically discussed combining both theoretical and experimental analysis. The specific anchoring sites in 2D host materials can be classified into two categories, 10 sub-categories (Figure 1E,F): metal-free materials consisting of carbonaceous materials and others such as black phosphorous, boron nitride, carbon nitride, and so forth, as well as metal-based materials including metals (alloys), metal

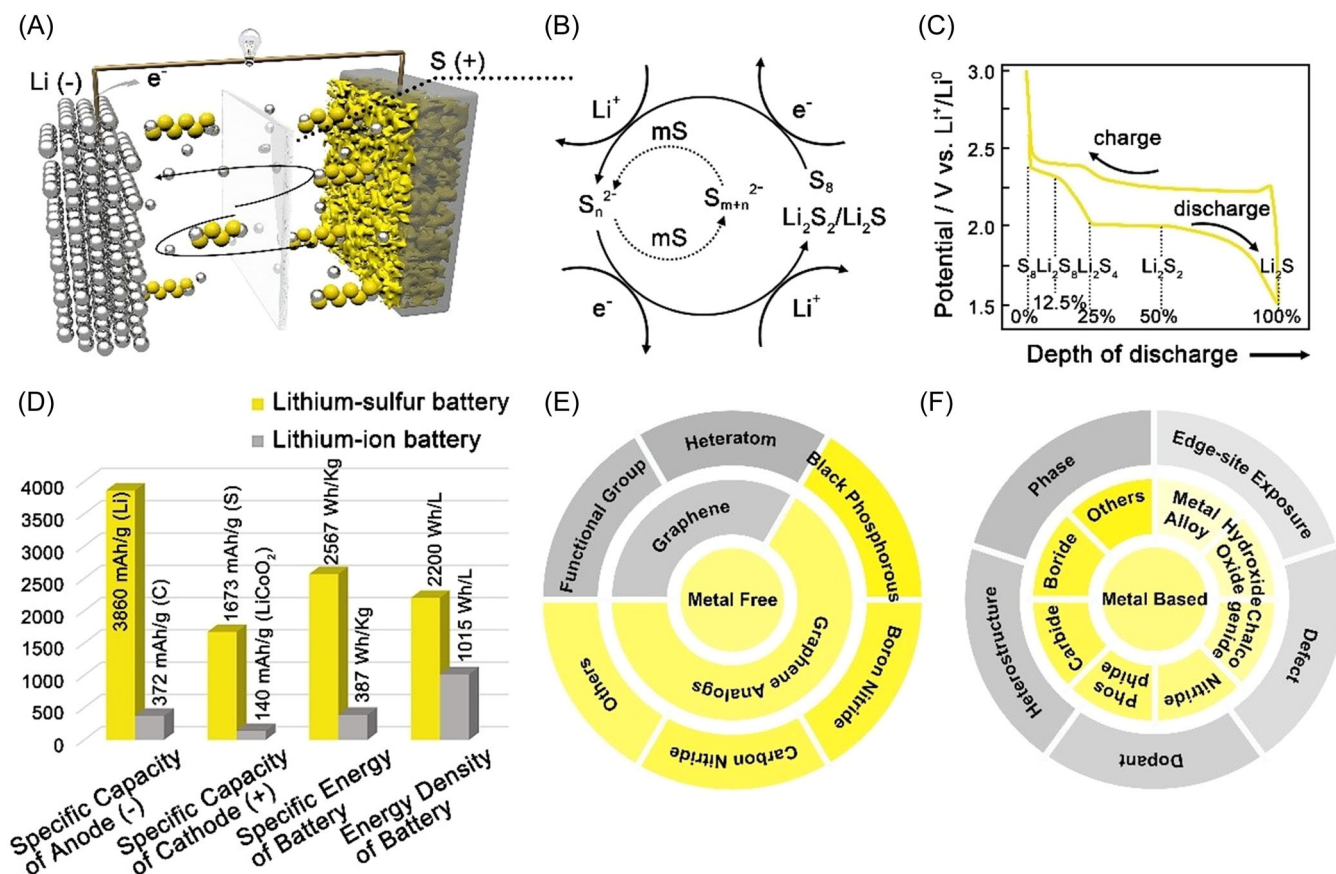


**FIGURE 1** (A) Schematic of Li-S battery. (B) Illustration of the typical sulfur conversion mechanism with the corresponding voltage profile shown as (C). (D) Summary of the important parameters of Li-S versus Li-ion battery. (E, F) Schematic illustration of metal-free and metal-based 2D materials applied in the current metal-sulfur battery.

oxides (hydroxides), metal chalcogenides, nitrides, phosphides, borides, carbides, and metal-organic frameworks. Significantly, we compare their advantages and disadvantages for application in metal-sulfur batteries, with an emphasis on efficient binding configuration for polysulfides adsorption/desorption. Finally, the key principles of building highly efficient coordination via defect engineering, dopant engineering, heterostructure, phase control, and their hybridization are remarked, which suggests an important guideline for the high-performance metal-sulfur battery in the future.

## 2 | MECHANISM OF METAL-SULFUR BATTERY

A significant development in the high-performance Li-S battery greatly enhances our understanding of sulfur redox chemistry, and thus accelerates the key transition from lab success to industry application.<sup>59–61</sup> Comparably, other alkalies or high-valent metal-sulfur batteries are still in their infancy, even though they share a similar conversion reaction as Li-S chemistry.<sup>12,17,62</sup> Here, we will emphasize on Li-S mechanism with main differences from others discussed as well. Being different from typical intercalation materials (i.e.,  $\text{LiFePO}_4$ ,  $\text{LiMn}_2\text{O}_4$ ), the S cathode proceeds through successive conversion reactions with metal anodes (i.e., Li, Na, K), separated by an ion-conducting liquid or solid electrolyte (Figure 1A).<sup>63–67</sup> Normally, stable-stacked sulfur formed by eight-atom rings ( $\text{S}_8$ ) are cleaved to embrace both lithium ions from electrolyte and electrons from the external electrical circuit, and thus reduced into a series of polysulfides until the formation of final sulfides, simply noted as follows:  $16\text{Li} + \text{S}_8 \rightleftharpoons 8\text{Li}_2\text{S}$  (Figure 1B,C).<sup>68</sup> It has been verified that the successive fracture-regeneration of the S-S bond is a very complex process of multiphase transfer involved with multi electrons.<sup>69</sup> During cell discharging, two plateaus are clearly seen in the galvanostatic voltage curve, which implies the gradual decrease in the sulfur chain length associated with phase transition.<sup>70,71</sup> The previous one occurring at 2.15–2.4 V indicates the reduction of sulfur to  $\text{Li}_2\text{S}_8$  and subsequently to  $\text{Li}_2\text{S}_6$  and  $\text{Li}_2\text{S}_4$ , featuring 0.5 electron transfer per sulfur atom and thus a theoretical capacity of 418 mA·h/g. Following, the lower discharge plateau at 2.1 V corresponds to the further reduction into highly insoluble and insulating lithium sulfides ( $\text{Li}_2\text{S}_2$  and  $\text{Li}_2\text{S}$ ), which utilizes 1.5 electrons transfer per sulfur atom and therefore leads to a theoretical capacity of 1254 mA·h/g. Although the cycling potential is quite lower than that of typical intercalation-based metal oxides, that is, around 3.2 V of  $\text{LiFePO}_4$  and 3.7 V of  $\text{LiMn}_2\text{O}_4$ , the highest capacity of

sulfur still correlates to very high energy densities of 2567 W·h/kg or 2200 W·h/L based on weight or volume, respectively (Figure 1D).<sup>72–74</sup>

Among diverse sulfur and sulfides resultant, high-order class (e.g.,  $\text{Li}_2\text{S}_n$ ,  $3 \leq n \leq 8$ ) are highly soluble in ether-based electrolytes, and then out-diffuse over separator into anode case, causing detrimental “shuttle effect” and severe loss of active materials. It is well recognized that the disproportionation or comproportionation equilibriums among different polysulfide species, such as  $\text{S}_8^{2-}$ ,  $\text{S}_6^{2-}$ ,  $\text{S}_4^{2-}$  and  $\text{S}_7^{2-}$ ,  $\text{S}_5^{2-}$ ,  $\text{S}_3^{2-}$ , are simultaneously occurring due to their close Gibbs free-energies.<sup>75,76</sup> The soluble high-order polysulfides  $\text{Li}_2\text{S}_n$  exhibit quite a poor reduction kinetics, causing severe concentration gradient and thus aggravating the shuttling effect.<sup>77</sup> This shuttling effect together with ineluctable side reaction is the major cause of serious capacity fading and excess use of electrolytes, which bottlenecks the practical use of the current metal-sulfur battery.<sup>72,78,79</sup> Yet, considering the poor electro/ion transfer derived from the insulating sulfur, the dissolution of polysulfides out of solid to liquid phase transition allows more active materials to participate in the electrochemical reaction.<sup>73,80</sup> Therefore, accelerating the conversion kinetics from long-chain to short-chain polysulfides upon discharging, and meanwhile, the reversible reaction into sulfur species upon charging, would minimize their dissolution issue, and thereby improve the sulfur utilization and battery performance.

In view of research studies over the past, collaborative efforts on cathode hosts designed to trap sulfur,<sup>2,81</sup> electrolyte modification to relieve shuttling effect,<sup>2,78,82</sup> and the application of functional interlayer to block transfer channel,<sup>20,78,83</sup> are needed toward the common goal. For instance, exploration of electrolytes reveals that carbonate solvents instead of ether-based electrolytes could relieve polysulfides shuttling, which is however chemically incompatible with most sulfur cathodes, merely except for pyrolyzed polyacrylonitrile sulfur composites and minor confined  $\text{S}_{2-4}$  in the microporous carbon matrix.<sup>84–88</sup> What is more, adding a functional interlayer for sulfur cathodes does help to buffer and block the shuttle route or speed up the redox reaction, while there is another issue to be considered, namely, the weight of the interlayer itself reduces energy density.<sup>89–92</sup> It seems that these methods fail to tackle the root cause responsible for the shuttling problem, namely the severe concentration gradient from kinetically-poor high-order polysulfides. By far, to optimize cathode architecture, two principles are prioritized: the first is to efficiently anchor polysulfides to reduce the shuttling impact, and the second is to catalyze sulfur redox reaction by lowering the conversion barrier.<sup>80</sup> Here, we encompass the main



advancement in the design of 2D polar cathodes with an emphasis on their chemically enhanced interaction with polysulfides. Through in-depth investigation combining both theoretical and experimental methodologies, the precise active sites with the optimized coordination for sulfur/sulfides regulation have been comprehensively described.

### 3 | METAL-FREE HOST MATERIALS

2D metal-free materials typically including g-C, g-CN, BN, and so forth, exhibit unparalleled advantages toward diverse applications regarding energy storage and conversion. For example, owing to its large specific surface area, high elastic modulus, and favorable thermal and electrical conductivity, graphene, the most studied 2D material, has become one of the intriguing materials to host sulfur. However, pure graphene is normally chemically inert which provides insufficient interaction toward chemically polar polysulfides, ultimately leading to quite limited cycling performance. Hence, more significant efforts have been devoted to surface modification to realize enhanced polysulfides trapping, such as functionalized graphene utilizing specific functional groups or heteroatoms, as well as other naturally polar graphene analogs (Figure 2). In this section, we first summarize key progress made in 2D carbonaceous host materials, with emphasis on their chemically polar interface design. Then, different graphene analogs, such as g-NC, BN, BP, and so forth are systematically illustrated. In general, the large fraction of chemically polar active sites across interfaces suggests an important role in their much better polysulfides regulation.

### 4 | FUNCTIONALIZED CARBON

Early research studies on sulfur cathode design are pioneered by the Nazar group ever since 2009, who put forward a proof-of-concept carbon framework, namely CMK-3, the most well-known member of the mesoporous carbon family (Figure 3A).<sup>72</sup> On it, the 6.5-nm-thick carbon rods separated by 3–4-nm-wide channel voids precisely constrain sulfur nanofiller growth within inner voids, thus giving rise to extremely high sulfur utilization of 84% and maintaining over 1000 mA·h/g discharge capacity for 20 cycles at 0.1 C. Inspired by this significant progress, diverse carbon hosts with high specific surface area as well as appropriate pore structure are well organized to physically restrain dissolved polysulfides rather than escaping from the cathode (Figure 3C).<sup>27,93–97</sup> Most recently, Cui and co-authors delicately design tortuous channel voids in highly tortuous graphene, which is utilized to extend the diffusion loss pathway of polysulfides and thereby mitigate their diffusion/dissolution loss (Figure 3B).<sup>98</sup> This material provides an approach to resolve the contradictory conflicts between ineffective trapping of large pores and limited loading caused by small pore volume. Consequently, an ultrahigh cathode areal capacity of 21 mA·h/cm<sup>2</sup> with 98.1% retention after 160 cycles can be achieved at 3.2 mA/cm<sup>2</sup>, largely surpassing the lower tortuosity counterpart. Also, it is identified that the sulfur-philicity surface ornamented by oxygen functional groups could consolidate bonding effects toward sulfur or sulfide species, thus further mitigating their outward loss.<sup>98</sup> Here, we focus on the main progress made on rational polar surface design enslaving certain functional groups (–OH, –COOH, –NH<sub>2</sub>, etc.) and heteroatoms (B, N, O, P, S, etc.), stressing

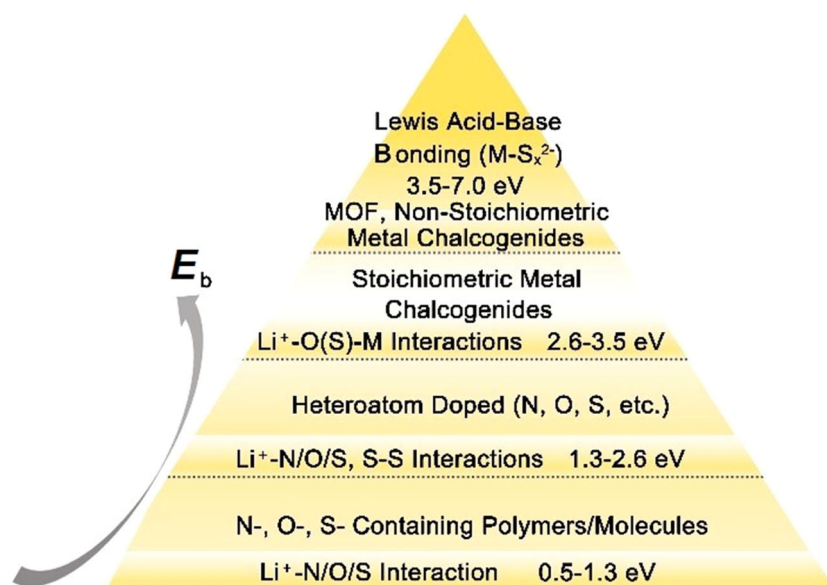


**FIGURE 2** Energy computation for diverse chemical adsorption toward lithium polysulfides.

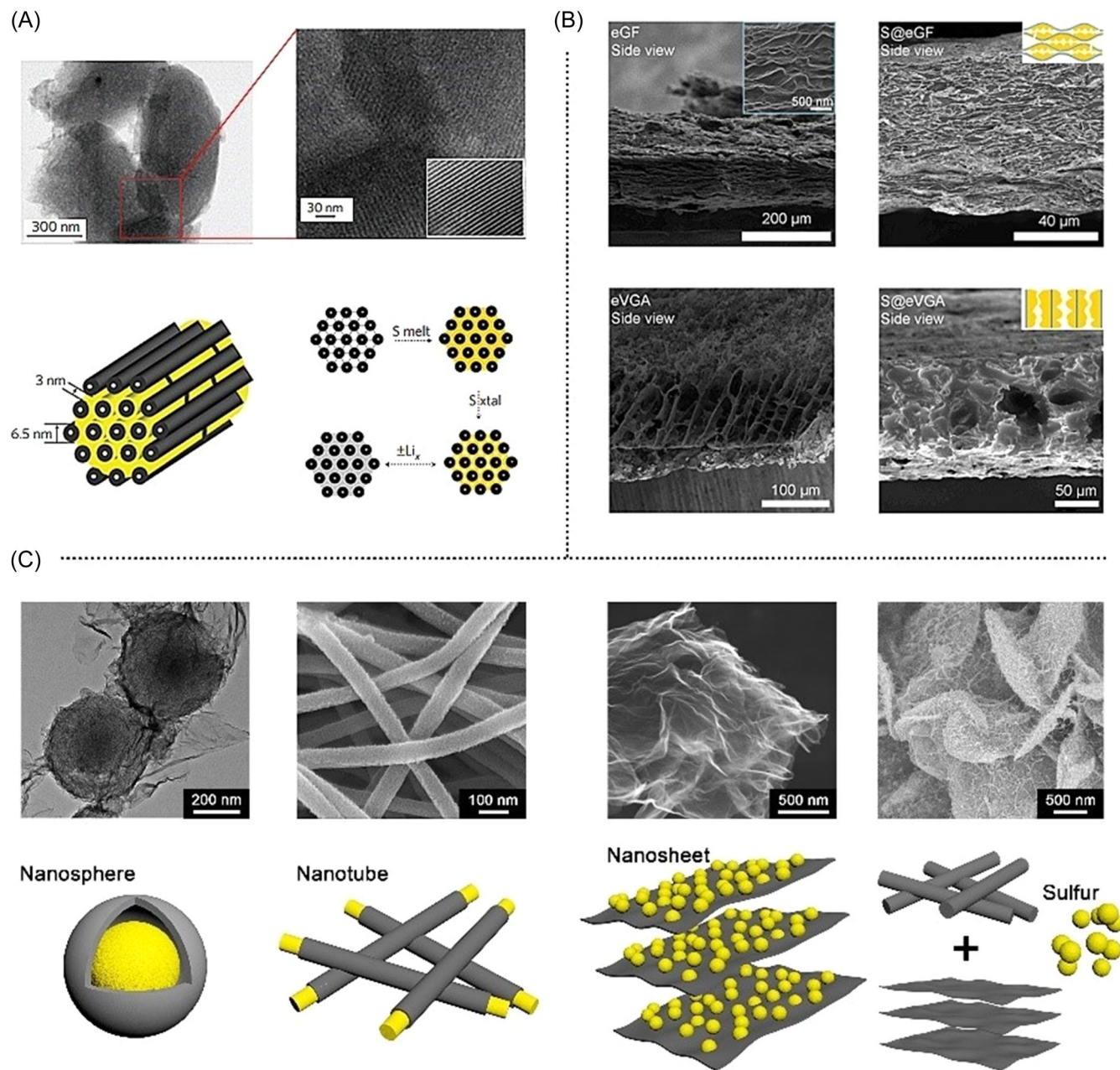


**FIGURE 3** Illustration of typical carbonaceous sulfur hosts: (A) CMK-3. Copyright 2009, *Nat. Mater.*; (B) High tortuosity rGO. Copyright 2020, *Matter*; (C) Typical carbon skeleton: carbon nanosphere, nanotube, nanosheet, and their hybrids. Copyright 2018, *Electrochim. Acta*, Copyright 2017, *Small*, Copyright 2020, *J. Phys. Energy*, Copyright 2012, *ACS nano*.

on their specific mechanism toward polysulfides inhibition.

## 5 | FUNCTIONAL GROUPS (–OH/–O–, –NH<sub>2</sub>, –SO<sub>3</sub>Ph, etc.)

Functional groups such as –OH/–O–, –NH<sub>2</sub>, –SO<sub>3</sub>Ph have been successfully introduced into carbonaceous skeleton as multifunctional modifiers to regulate electron distribution and physiochemical character. The key role

is charge redistribution causing a chemically polar interface for enhanced polysulfides trapping. For example, Zhang and co-workers perform ab initio calculation to clarify that epoxy and hydroxyl functional groups grafted onto graphene enhance the binding of S atoms to C–C bonds due to induced ripples by these functional groups.<sup>37</sup> X-ray absorption spectroscopy (XAS), a powerful tool for probing unoccupied electronic structures, is used to determine the origin of chemical interaction and thus anchoring effect at the heterogeneous surface.<sup>99–101</sup> Carbon K-edge absorption spectra in Figure 4A detect the



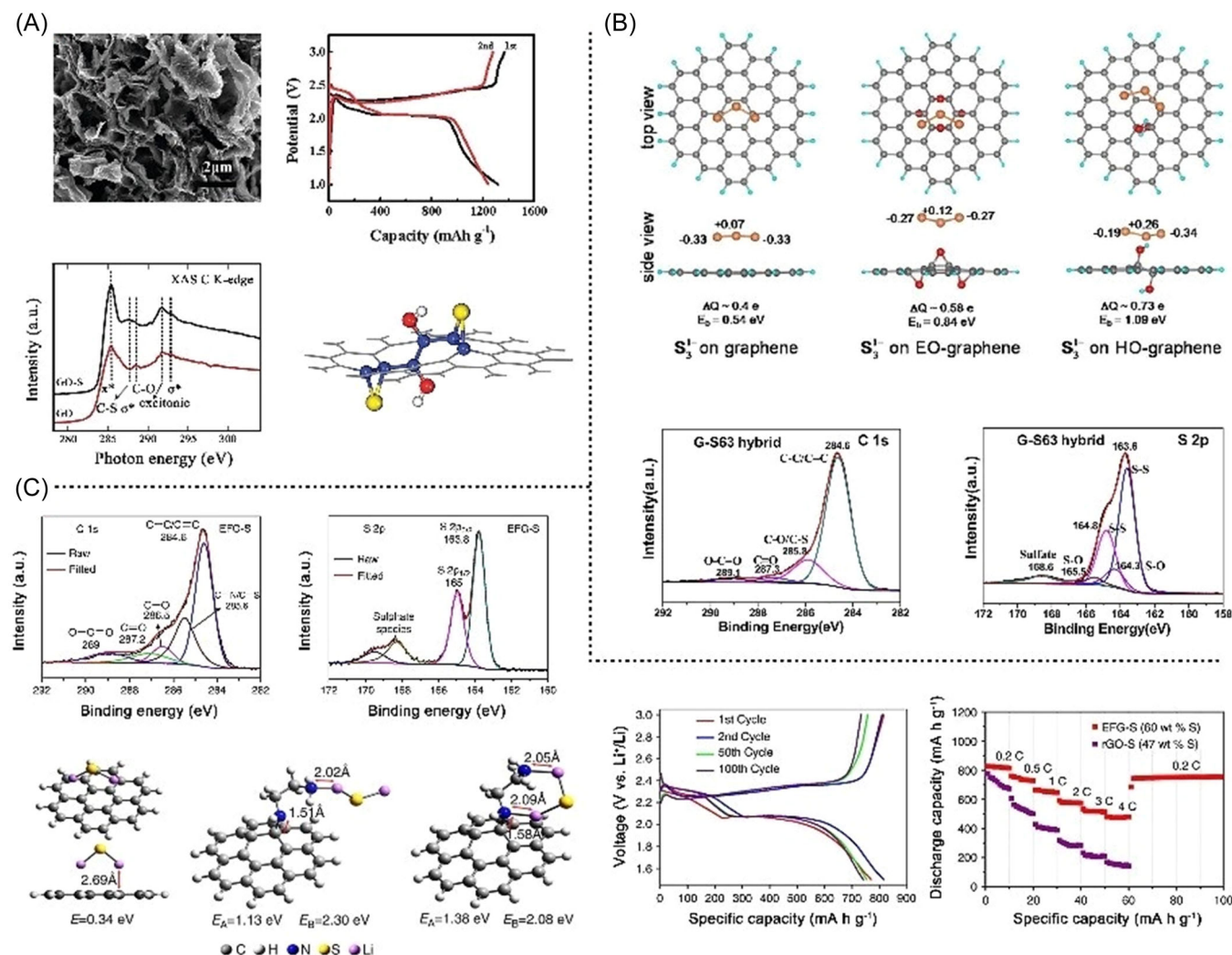


**FIGURE 4** Functional groups decorated graphene: (A) –OH/–O– induces ripples on graphene's six-membered ring structure and thus enhances the binding of S to the C–C bond. Copyright 2011, *J Am Chem Soc*; (B) –OH induces more asymmetrical charge distribution, and larger polarization as well as stronger electrostatic interaction than –O– groups. Copyright 2013, *ACS Nano*; (C) –NH<sub>2</sub>– enables the formation of N–Li and C–S binding. Copyright 2014, *Nat Com*.

significantly weakened C–O bond possibly derived from charge redistribution when incorporated with S. Meanwhile, a new feature originating from the C–S σ\* excitations is observed, implying chemically enhanced interaction between active C atoms with polysulfide intermediates, while the increase in the sharpness of the sp<sup>2</sup>-hybridized carbon structure is better formatted after S incorporated.<sup>37</sup> These highly reactive functional groups over graphene efficiently immobilize the S cathode and thus deliver a good performance of high reversible capacity of 950–1400 mA·h/g at 0.1 C.<sup>37</sup> Additionally, Cheng's team dissects the precise mechanism of how oxygen-containing (primarily hydroxyl/epoxide) groups adsorb polysulfides molecules and thus further distinguishes their various effects. It is discovered that

introducing hydroxyl and epoxide functional groups enables charge transfer from polysulfide anions to graphene, thus remarkably increasing their binding energy. Besides, hydroxyl groups on the graphene surface can induce more asymmetrical charge distribution on the two end sulfur atoms, resulting in larger polarization and consequently stronger electrostatic interaction over than epoxide-graphene (Figure 4B).<sup>102</sup>

In addition to the epoxy and hydroxyl groups, other functional groups such as –NH<sub>2</sub>–/–SO<sub>3</sub>Ph are also well developed to modulate the bonding effect at the sulfur–carbon interface.<sup>103–105</sup> For example, the Lou group report amino functionalized reduced graphene as a feasible and effective sulfur host to solve the long-term cycling difficulty.<sup>103</sup> Ethylenediamine with two electron-donating amine groups on the carbon aliphatic spacer is

applied as an ideal crosslinker to covalently join polar lithium sulfides and nonpolar carbon surfaces together. Experimental results and theoretical analysis show that amino moieties strongly interact with discharge products in two different ways (Figure 4C), therefore contributing to a stable capacity retention of 80% for 350 cycles with high capacity and excellent high-rate response up to 4 C. To conclude, introducing functional groups onto graphene can not only increase the reactivity of aromatic carbon rings toward sulfur and sulfides species but also directly interact with them based on enhanced covalent binding. Although it lessens polysulfides dissolution and diffusion in a prolonged cycle span, additional problems, such as compromised electron/ion migration particularly in high-proportion circumstances, must be considered.

## 6 | HETEROATOMS (B, N, O, P, S, etc.)

By contrast, through relocating heteroatoms (such as B, N, O, P, or S) into carbon-defect sites, the C-C lattice can be restored, resulting in improved electron transferability. Additionally, their discrepant electronegativity from carbon atoms gives rise to a stronger interaction with metal cations, which is essential for effectively trapping higher-order polysulfides.<sup>106–113</sup> Early studies about the essential role of heteroatoms in carbon are concentrated on N-doped graphene. Zhang group compares bond variation before and after cycling via XAS measurement; it is found that at the fully discharged state, the C-S bond feature disappears in the S K-edge spectrum, and a new peak at 398.5 eV emerges in the N K-edge spectrum, which is quite different from previous observation from oxygen-functional carbon. This could be ascribed to the lithiation of S to  $\text{Li}_2\text{S}_2$  or  $\text{Li}_2\text{S}$  and the formation of N... $\text{Li}_2\text{S}_x$  interactions (Figure 5A).<sup>106</sup> Later, Zhang and co-workers identify this Li bond in sulfur cathodes through sophisticated quantum chemical calculation combined with  $^7\text{Li}$  nuclear magnetic resonance (NMR) spectroscopy. They propose for the first time a quantitative descriptor of chemical shift in  $^7\text{Li}$  NMR to describe the Li-bond strength and significantly such strong dipole-dipole interaction from electron-rich donor N atoms can be largely enhanced by the inductive and conjugative effect from scaffold materials with  $\pi$  electrons (e.g., graphene) (Figure 5B).<sup>114</sup> Besides, Wang et al. demonstrate novel mesoporous nitrogen-doped carbon/sulfur nanocomposites as cathode enable excellent cycling stability in Li-S chemistry (95% retention within 100 cycles at a high current density of  $0.7 \text{ mA}\cdot\text{h}/\text{cm}^2$  with a high sulfur loading of  $4.2 \text{ mg}/\text{cm}^2$ ) (Figure 5C).<sup>111</sup> In-depth investigation combining XANES

and theoretical simulation confirm nitrogen dopants can change the electronic structure of nearby oxygen atoms in the doped carbon framework thus to promote the chemical interaction of the oxygen with sulfur (Figure 5C). Similarly, other heteroatoms such as B, O, P, and S are also introduced as modulator centrals to modify electronic localization neighboring heteroatoms. To elaborate on the specific mechanism of how different doping atoms including B, N, O, F, P, S, and Cl affect the adsorption capability, the Li group conducts a systematical density functional theory calculation over this heteroatoms-doped nanocarbon. It is proved that the chemical modification using N or O dopant significantly enhances the interaction between the carbon hosts and the polysulfides, while the introduction of B, F, S, P, and Cl monodopants into the carbon matrix is unsatisfactory and at this circumstance, codoping is more favorable to facilitate a better anchoring effect (Figure 5D).<sup>112</sup> To conclude, heteroatom doping is utilized to enhance the chemical adsorption of highly polar hydrophilic polysulfides onto the nonpolar hydrophobic carbon matrix and consequently leads to better rate performance and cycling life. Yet, low-content heteroatoms usually have a limited effect on the entire interface, and hence long-term cycling behavior remains unsatisfactory in terms of practical requirements, particularly in high-loading circumstances.<sup>23,55</sup>

## 7 | P, BN, g- $\text{C}_3\text{N}_4$ , AND SO FORTH

Some graphene analogs, such as g- $\text{C}_3\text{N}_4$ , BN, P, and others, have found extensive use in diverse applications, including field nano emitters, nanoelectronics as well as composite reinforcement.<sup>41,42</sup> With respect to metal-sulfur batteries, they serve as a functional interface to absorb polysulfides via stronger electrostatic coupling and even decrease the charge transfer resistance to accelerate their conversion rate as well.<sup>115–119</sup> Phosphorene, one typical 2D layered material, offers a direct band gap between the zero gap of graphene and the large band gap from 2D transitional metal dichalcogenides, showing great potential for energy storage application. On it, each phosphorus atom bonds with three neighboring atoms forming a puckered honeycomb structure. Recently, Koratkar et al. incorporate few-layer phosphorene into a porous carbon as the cathode matrix to load sulfur, which enables the desirable performance of above  $660 \text{ mA}\cdot\text{h}/\text{g}$  after 500 cycles at 0.2 C with only  $\approx 0.053\%$  capacity decay per cycle (Figure 6A).<sup>116</sup> Theoretical calculation indicates the responsible reason that can be ascribed to enhanced polysulfides immobilization derived from the higher binding energy of 1–2.5 eV,



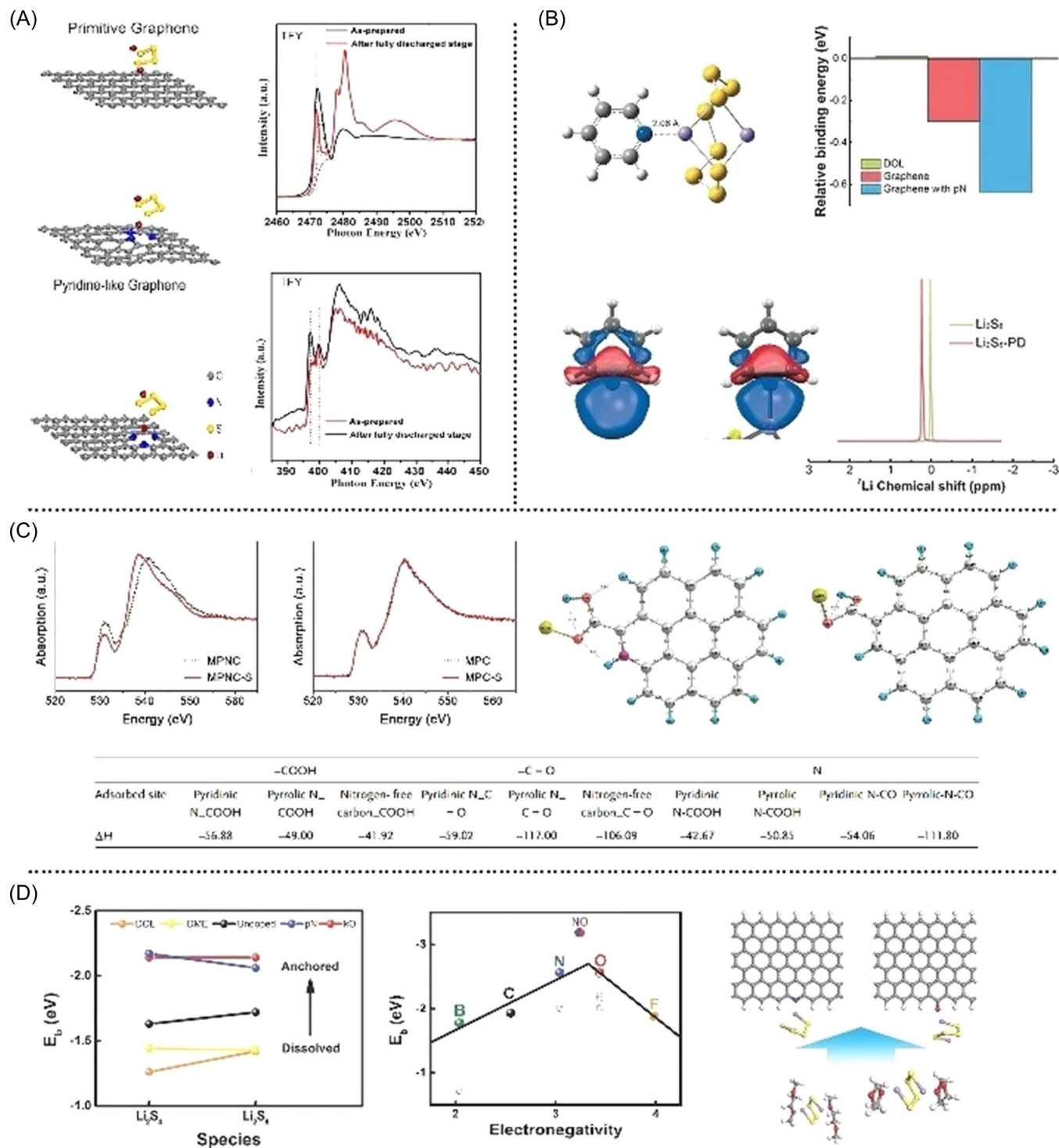


**FIGURE 5** Heteroatom dopants functionalized graphene: (A) C-S bond disappears along with the formation of N...Li<sub>2</sub>S<sub>x</sub>. Copyright 2014. *Nano Lett.*; (B) Both electron-rich donor N, as well as the inductive and conjugative effect, realize enhanced Li bind. Copyright 2017. *Angew Chem Int Ed*; (C) N dopants promote the adsorption of sulfur on oxygen functional groups. Copyright 2014. *Adv Funct Mater*; (D) Binding energy comparison across various atoms dopants over carbon, including B, N, O, F, P, S, and Cl. Copyright 2016. *Small*.

compared with only 0.5 eV of the carbon hexatom network (Figure 6A). The g-C<sub>3</sub>N<sub>4</sub> with 2D graphene-resembling structure is made up of tri-s-triazine networks joined by planar amino groups, which claim a

stronger affinity for sulfur/sulfides species owing to the large concentration of chemically polar pyridinic-N sites. Guo and co-worker use microemulsion-assisted assembly approach to prepare a 3D porous S/g-C/g-C<sub>3</sub>N<sub>4</sub>

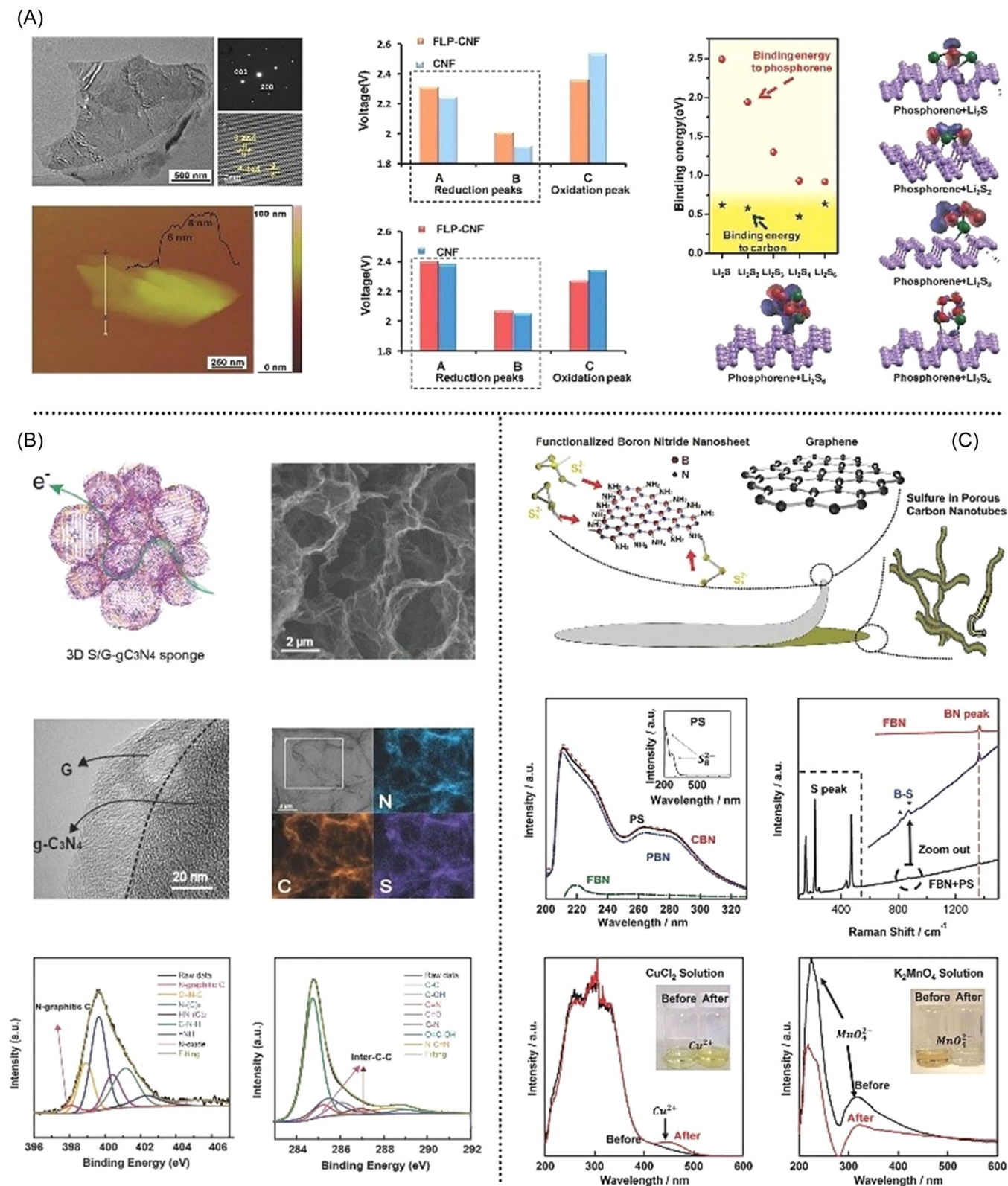


FIGURE 6 Illustration of typical graphene analogs sulfur hosts: (A) Phosphorene nanosheets. Copyright 2016. *Adv Mater*; (B) Carbon nitride nanosheets. Copyright 2018 *Adv Energy Mater*; (C) Boron nitride nanosheets. Copyright 2018 *Adv Energy Mater*.

free-standing cathode, which can deliver a superior cycling performance of 612 mA·h/g at 10 C under high sulfur loading of 82 wt%. On it, the enriched N-sites in g-C<sub>3</sub>N<sub>4</sub> macropores offer numerous adhesion sites for polysulfides, realizing a “physical-chemical” dual-confinement for polysulfides from diffusion (Figure 6B).<sup>120</sup> BN nanosheets isoelectronic with graphene embrace many remarkable properties such as high resistance to oxidation and good chemical inertness. Recently, Chen group used the solid-state ball milling method to fabricate amino groups functionalized BN/graphene as a conductive interlayer to decrease the charge transfer resistance and mitigate the shuttling problem. As verified, the positively charged amino groups –NH<sub>2</sub>– play an important role in the adsorption of polysulfides anion ions. Besides, the appearing B-S bands in Raman reveal their enhanced interaction between BN and sulfur/sulfides family (Figure 6C).<sup>115</sup>

## 8 | METAL-BASED ACTIVE CENTRALS

Owing to the high physicochemical diversity and chemical activity, metals and metal compounds, such as transitional metal oxides/hydroxides/chalcogenides/nitrides/phosphides/carbides/borides, are explored as catalytical centrals to govern redox reactions in a variety of energy storage and conversion system.<sup>121–123</sup> Toward metal–sulfur battery, they are recognized as chemically active locations for not only enabling homogenous sulfur deposition but also restraining dissolved polysulfides. More importantly, most metal/metal mixtures show the rewarding capability to catalyze sulfur redox reactions by decreasing the conversion energy barrier. Such accelerated reaction kinetics is crucial to guarantee more reversible metal–sulfur chemistry, especially at key steps where inadequate conversion of soluble long-chain sulfides into insoluble short-chain sulfides causes a concentration gradient and hence exacerbates the shuttling effect and capacity loss.<sup>124,125</sup> Transitional metal compounds, however, are frequently restricted by high charge transfer resistance, necessitating an additional step of surface diffusion to proceed with the overall process, considerably impairing their function as catalysts to accelerate conversion rates. Moreover, the reduced specific area from aggregated 2D layer structure paired with a higher mole rate often leads to a significantly lower specific energy density. One solution for this is to develop rational carbon/metals or metal compounds composite electrodes, while another is to shrink the size of metals and metal compounds into even

atomic clusters. In this section, we summarize the recent exciting progress toward 2D metal-based active centrals in metal–sulfur batteries, which can be categorized into eight classes such as metal/metal alloy, metal oxides/hydroxides, metal chalcogenides, metal nitrides, metal phosphides/carbides/borides, MXenes as well as the metal-organic framework.

## 9 | METAL/METAL ALLOY

Pt, Co, Ni, and so forth-containing metals and metal alloys have been widely used in catalysis, batteries, fuel cells, and supercapacitors.<sup>47,94,126,127</sup> While applied in metal–sulfur battery, they are proposed to speed up the conversion reaction of soluble polysulfides into insoluble sulfur (during the charge process) or disulfides (during the discharge process), thus easing the shuttling effect. Recently, single-atom catalysts (SACs), well-dispersed on carefully designed carbonaceous substrates, have attracted growing interest in promising sulfur cathode design. SACs can maximize the utilization of exposed metal atoms due to the downsizing of metals to the atomic level, therefore lowering the required metal content and reducing the cost compared to other metal/metal alloys. In addition, due to their distinctive highest energy occupied and lowest energy unoccupied molecular orbital gaps, SACs display high polarity, which provides a strong affinity toward polysulfides. Working synergistically with advantages from 2D layered carbonaceous substrates, such as large specific surface area and fast electron/ion conductivity, as obtained SACs/sulfur cathodes demonstrate relieved “shuttle effect” and facilitated reaction kinetics, to simultaneously improve the energy density, rate performance, and cycle life. Until now, various single metal atoms have been successfully confined into nitrogen-doped carbon to form the most popular M–N–C (M = Pt, Co, Ni, Al, V, Fe, Mn, Ru, and Zn) coordination as catalytically active sites to regulate polysulfides. In addition to the coordination effect of N and C species through  $\sigma$ -bonds, the N species serve to coordinate the metal atoms at the edge or defective sites of the graphitic domain. For example, the auspicious Pt catalysts are uniformly dispersed over the layered functionalized graphene by NaBH<sub>4</sub> solution-reduction, at which spatial distribution of metallic nanoparticles about 20 nm in size is observed (Figure 7A).<sup>47</sup> XPS results witness the formation of insoluble Li<sub>2</sub>S and Li<sub>2</sub>S<sub>2</sub> at the end of both discharge and charged states of bare graphene electrode, which indicates poor reversibility of deposited short-chain polysulfides to long-chain polysulfides. By contrast, a significant reduction is



observed for the charged state of Pt/Graphene electrode and thus illustrates better reversibility. Apart from precious metal, nonprecious cobalt atoms embedded into nitrogen-doped graphene are also applied to trigger the surface-mediated redox reaction of lithium polysulfides (Figure 7B).<sup>94</sup> A combination of operando XAS and first-principles calculation reveals that the Co-N-C coordination centers serve as a bifunctional electrocatalyst to facilitate both the formation and the decomposition of  $\text{Li}_2\text{S}$  in the discharge and charge processes, respectively. Nevertheless, large-scale synthesis of single-atom catalysts with high-loading remains a major bottleneck in current research owing to the difficulty of such atomic-level precision. A potential route is to rationally design suitable support materials for the uniform distribution of single atoms, such as defect-modified nanomaterials.

## 10 | METAL OXIDES/HYDROXIDES

In contrast to graphene or graphene analogs, transitional metal compounds potentially have stronger adsorption capability and more complex adsorption mechanisms toward polysulfides, due to their more ionic-bond feature closely associated with higher chemical polarization. Typically, low-cost 2D metal oxides like  $\text{Al}_2\text{O}_3$ ,  $\text{SiO}_2$ ,  $\text{TiO}_2$ ,  $\text{VO}_2$ ,  $\text{V}_2\text{O}_3$ ,  $\text{V}_2\text{O}_5$ ,  $\text{MnO}_2$ ,  $\text{Fe}_3\text{O}_4$ , and  $\text{MoO}_3$  are thoroughly investigated and make substantial progress toward the high-performance metal-sulfur battery.<sup>128</sup> However, suffering from limited electric conductivity, they often function in conjunction with diverse carbon matrices to ensure both ion and electron transferring, thereby increasing their utilization. As reported, for those non-conductive metal-oxides, the absorbed  $\text{Li}_2\text{S}_x$  should be

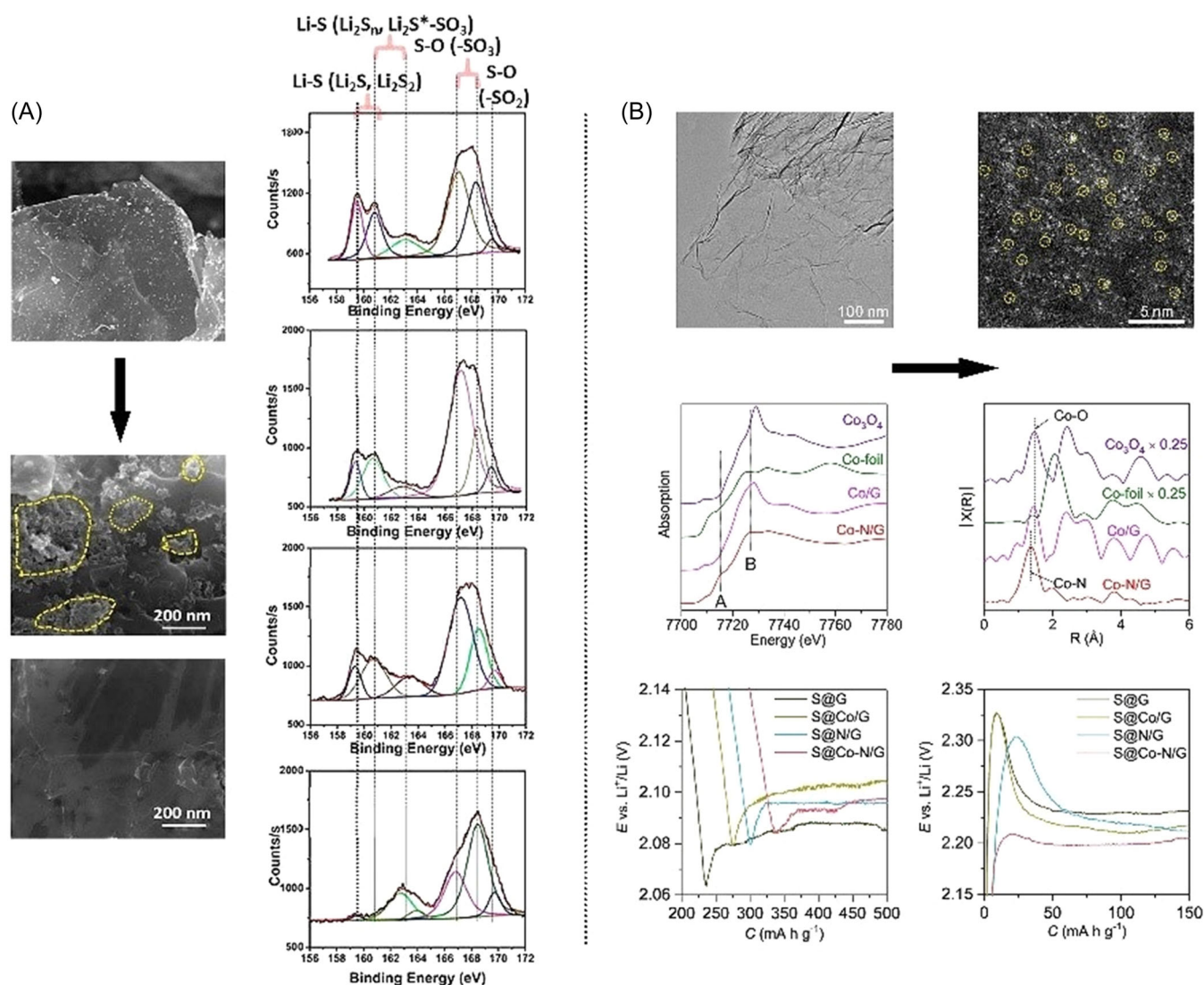
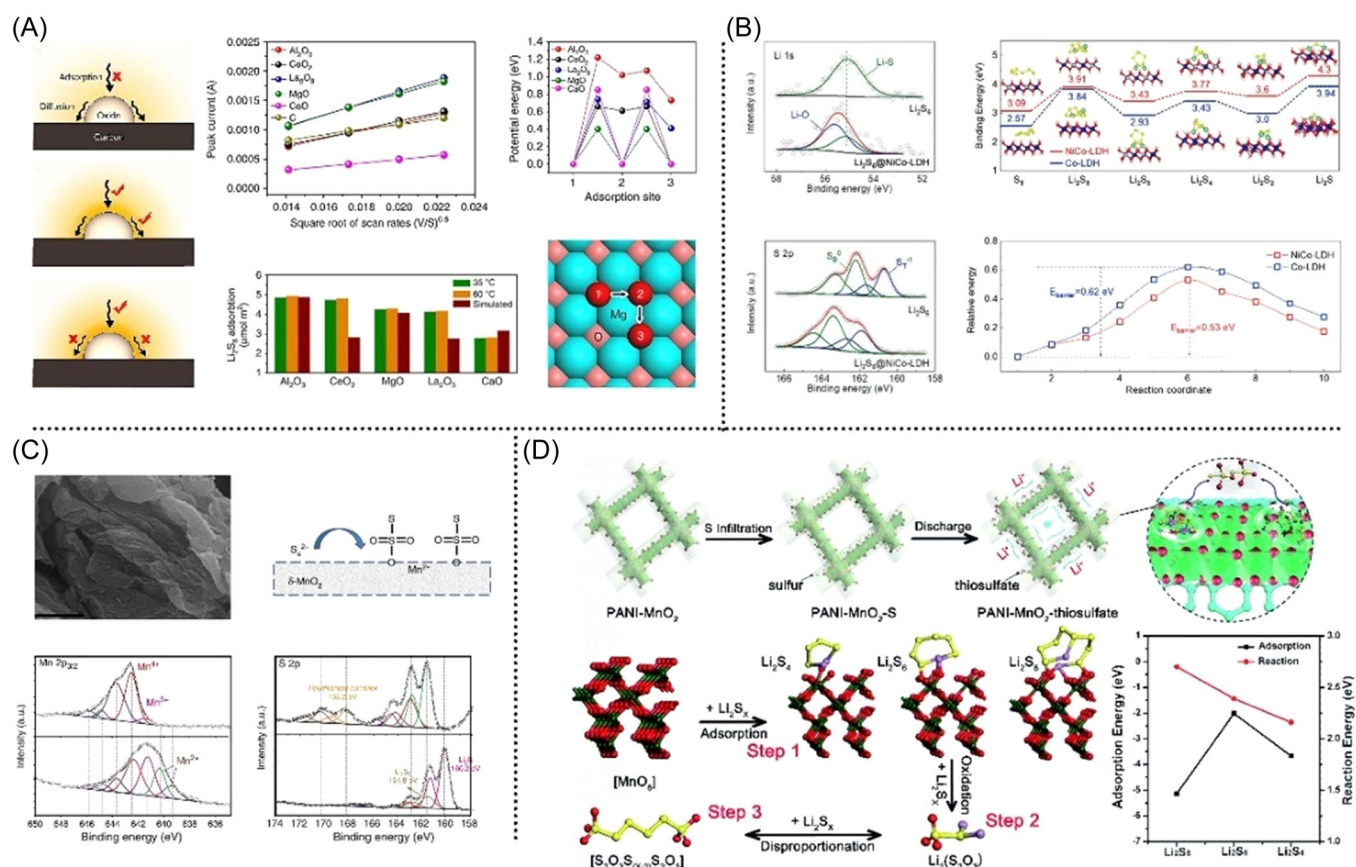


FIGURE 7 Metal single atoms: (A) Pt clusters over graphene electro-catalyze complete polysulfide redox. Copyright 2015. *J Am Chem Soc*; (B) Co single atoms grown on N doped graphene endow Co-N-C catalytical sites. Copyright 2019. *J Am Chem Soc*.



transferred from the surface of the oxide to the conductive carbon substrate to undergo the electrochemical reaction, otherwise, the conversion efficiency will be largely compromised. Cui and co-workers design various non-conductive metal oxides ( $\text{MgO}$ ,  $\text{Al}_2\text{O}_3$ ,  $\text{CeO}_2$ ,  $\text{La}_2\text{O}_3$ , and  $\text{CaO}$ ) nanoparticles-decorated carbon flakes as sulfur hosts via a facile and generic bio-templating method using Kapok trees fibers as both the template and the carbon source (Figure 8A).<sup>129</sup> Adsorption test, microstructure analysis and electrochemical performance evaluation combined with density functional theory calculations reveal better surface diffusion from  $\text{MgO}$ ,  $\text{CeO}_2$  and  $\text{La}_2\text{O}_3$  sulfur cathodes, which therefore show higher capacity and better cycling stability.<sup>129</sup> Resembling the metal oxides, hydroxides are also implemented as important polysulfide reservoirs to realize a highly stable sulfur cathode. More recently, the Chen group well developed unique hierarchical micro-nano architecture composed of bimetallic NiCo-layered double hydroxide for sulfur trapping. Compared to the mono-metallic Co-layered double hydroxide counterpart, the introduction of secondary metal intensifies the chemical interactions between the host-guest interface, which

implements strong sulfur immobilization and catalyzation for rapid and durable sulfur electrochemistry (Figure 8B).<sup>130</sup> Generally, the polysulfide capture by the oxides/hydroxides is via monolayered chemisorption between anion and cation, and in some case, the too strong binding energy of Li-O bond made it difficult to break out somewhat hindering the further reduction. Apart from such a chemisorption mechanism, some instead rely on emerging surface-bound intermediates to trap polysulfides. A typical example is manganese dioxide nanosheets, one kind of very poor semiconductor, which functions as a redox shuttle to catenate and bind “higher” polysulfides and meanwhile convert them into insoluble oxidation via disproportionation (Figure 8C).<sup>128</sup> As reduction proceeds, the surface thiosulfate groups are proposed to anchor newly formed soluble polysulfides, which therefore curtails active mass loss during the discharge/charge process and suppresses the polysulfide shuttle so as to result in high-performance cathodes with high sulfur loading. Another research on exploring  $\text{MnO}_2$ -mediated redox reaction is conducted by Su and so forth. and they report the reduced oxidation state of Mn occurs along with



**FIGURE 8** Metal oxides/hydroxides: (A) Comparison in nonconductive metal oxides  $\text{MgO}/\text{Al}_2\text{O}_3/\text{CeO}_2/\text{La}_2\text{O}_3/\text{CaO}$  distinguishes the important role of surface diffusion. Copyright 2015. *Nat Comm*; (B) NiCo-layered double hydroxides allow for the formation of the Li-O bond. Copyright 2021. *Adv Sci*; (C)  $\text{MnO}_2$  reacts with initially formed lithium polysulfides to form surface-bound intermediates. Copyright 2014. *Nature Comm*; (D)  $\text{MnO}_2$  allows for the formation of polythiosulfates in cycled  $\text{MnO}_2/\text{Li}_2\text{S}_4$ . Copyright 2020. *J Mater Chem A*.

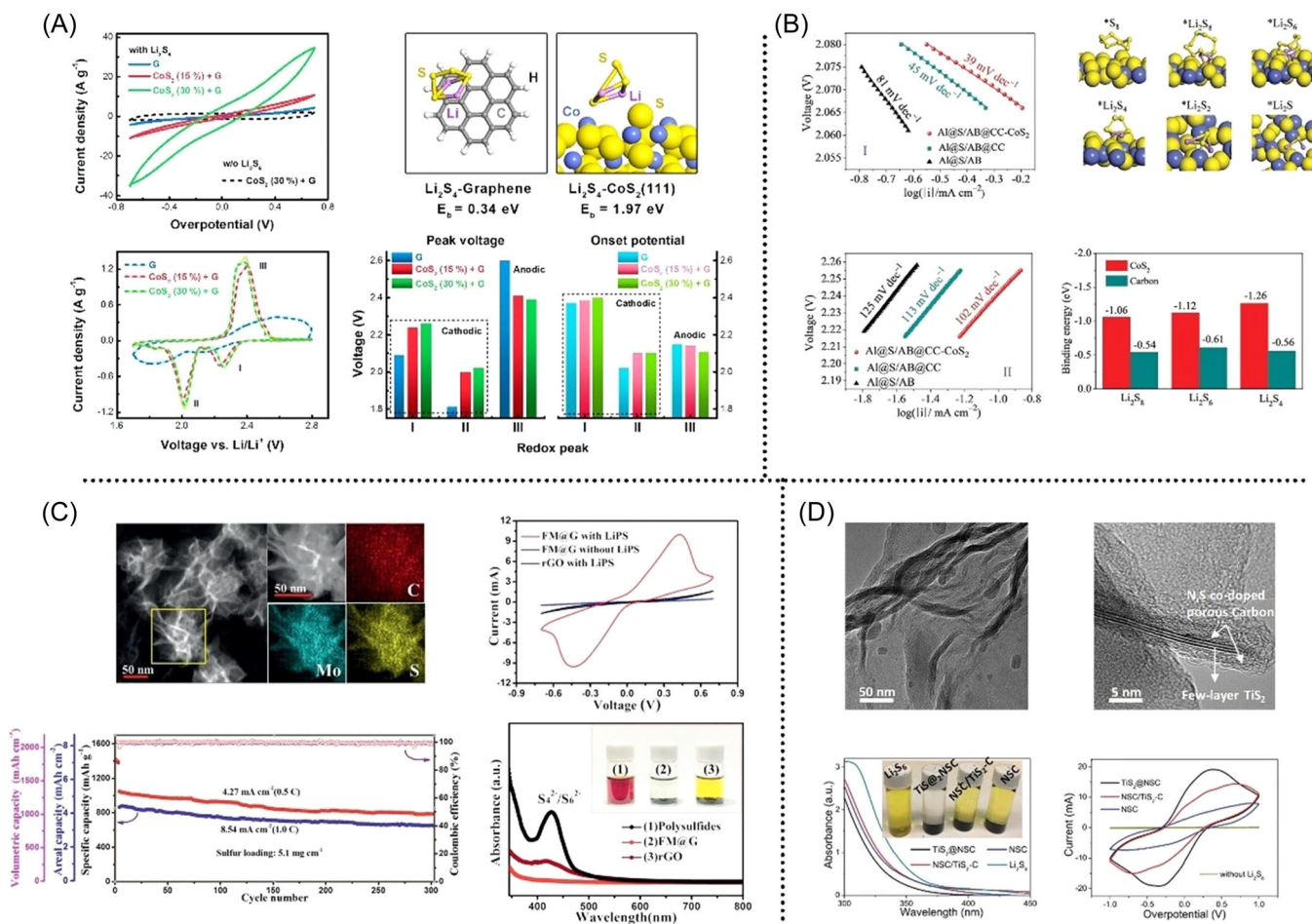


**FIGURE 9** Metal chalcogenides: (A) CoS<sub>2</sub> sulfiphilic hosts. Copyright 2016. *Nano Lett*; (B) CoS<sub>2</sub> functionalized carbon cloth. Copyright 2021. *Adv Sci*; (C) MoS<sub>2</sub> decorated graphene. Copyright 2021. *Adv Energy Mater*; (D) TiS<sub>2</sub> confined in N, S codoped carbon. Copyright 2019. *Adv Energy Mater*.

the oxidation of Li<sub>2</sub>S<sub>4</sub> into polythiosulfates in cycled MnO<sub>2</sub>/Li<sub>2</sub>S<sub>4</sub>. This verifies MnO<sub>2</sub> nanoparticles not only have strong adsorption capacity for polysulfides but also play a “catalytic” role during the charge/discharge process (Figure 8D).<sup>131</sup> Although polar transitional metal oxides could effectively boost the dynamics of polysulfides transformation and deposition of Li<sub>2</sub>S, their poor electrical conductivity increases the battery resistance and lowers the rate capability. It commonly necessitates the use of a large amount of electrochemically inactive conductive carbon to improve the utilization of the active materials, thereby lowering overall cathode energy density.

## 11 | METAL CHALCOGENIDES

Metal chalcogenides, commonly consisting of transition metals coupling by S, Se, or Te, and so forth, are emerging as another significant class to control sulfur dissolution/precipitation in the metal–sulfur cell.<sup>44,132–137</sup> Taking metal

sulfides for example, just similar to their oxide counterparts, binding polysulfides onto their surface is ascribed to both positive metal centrals and negative sulfur ions with diverse coordination. Usually, the metal atom centers with modified electronic distribution give rise to enhanced binding sites for sulfide anions from extrinsic adsorbates, while the soft basic for example, S<sub>2</sub><sup>2-</sup> ions covalent nature renders decent electrical conductivity, both of which show significant aid in maintaining high-capacity retention. Over the past, exploring chemically reactive metal sulfides as host materials has become increasingly popular and is crucial for controlling polysulfides, with typical examples including TiS<sub>2</sub>, VS<sub>2</sub>, Co<sub>x</sub>S<sub>y</sub>, ZrS<sub>2</sub>, Mo<sub>x</sub>S<sub>y</sub>, WS<sub>2</sub>, Ni<sub>3</sub>S<sub>2</sub>, Sb<sub>2</sub>S<sub>3</sub>, and so forth. Cobalt disulfide, one of the most studied metal disulfides, with appreciable conductivity and large surface area, is verified as a credible host material to load sulfur. Due to the intimate contact via S<sub>n</sub><sup>2-</sup>-Co<sup>δ+</sup> and Li<sup>+</sup>-S<sup>δ-</sup> binding, much desirable electrochemical performance over a long time span can be guaranteed.<sup>138</sup> Zhang and coauthors prepared highly crumpled CoS<sub>2</sub>/graphene as

sulfur substrates, which shows both high trapping capability and remarkable electrocatalytic activity for their redox reaction (Figure 9A).<sup>134</sup> More rewardingly, half-metallic CoS<sub>2</sub> possesses an appreciable conductivity of  $6.7 \times 10^3$  S/cm at 300 K, which far exceeds those of other semi-conducting first-row transition metal disulfides such as FeS<sub>2</sub> and NiS<sub>2</sub>, affording efficient electron pathways and high electrocatalytic activity. The accelerated polysulfides redox kinetics, confirmed by electrochemical evidence, promises low polarization and high energy efficiency under high current densities, as well as excellent cyclic performance.<sup>134</sup> Most recently, Lu and coworkers cover CoS<sub>2</sub> onto carbon cloth, working as both three-dimensional current collector and physicochemical barrier to retard the migration of soluble polysulfides (Figure 9B).<sup>139</sup> As constructed, the cathode exhibits efficient physical blocking, strong chemisorption, and fast catalytic redox reaction kinetics in sulfur chemistry.<sup>139</sup> Apart from CoS<sub>2</sub>, MoS<sub>2</sub>, another representative 2D metal chalcogenide, is also widely studied. Recently, the Zhang group reported metallic 1T-MoS<sub>2</sub> decorated graphene, acting as both the cathode and separator modifier, exhibits superior cyclability with a capacity retention of 71.7% over 500 cycles (Figure 9C).<sup>140</sup> Importantly, steady cyclability and high volumetric capacity of 1360 mA·h/cm<sup>3</sup> with a high sulfur loading of 5.1 mg/cm<sup>2</sup> are also attained even at a high current density of 4.27 mA/cm<sup>2</sup>.<sup>140</sup>

Besides, even the reliable synthesis is still challenging due to the strong tendency of stacking and oxidation, 2D TiS<sub>2</sub>, as the lightest member of transition metal dichalcogenides, still holds great promise as an appealing sulfur host. More recently, Wang et al. demonstrate for the first time the successful conversion of Ti<sub>3</sub>C<sub>2</sub>T<sub>x</sub> MXene to sandwich-like ultrathin TiS<sub>2</sub> nanosheets confined by N, S co-doped porous carbon via an in situ polydopamine-assisted sulfuration process (Figure 9D).<sup>141</sup> Meanwhile, the polydopamine coating is utilized to suppress the strong tendency of stacking and oxidation of ultrathin TiS<sub>2</sub> nanosheets. While used as a sulfur host in the Li-S battery, they show both high trapping capability for lithium polysulfides, and remarkable electrocatalytic activity for the reduction and oxidation process. Particularly, high-quality operando synchrotron XRD was conducted to gain insight into the sulfur transformation and lithiation/delithiation of the working cell. The XRD patterns show that the intensity of S<sub>8</sub> peaks decreases and completely disappears in the last part of the low discharge plateau, while no Li<sub>2</sub>S peak is detected along with the discharging, and during charging no crystalline S<sub>8</sub> peak is observed. Such absence of Li<sub>2</sub>S/S<sub>8</sub> crystals instead of the formation of amorphous phases can be also attributed to the high surface area and catalytic activity of TiS<sub>2</sub>, where the sulfur species can be homogeneously distributed and utilized

without aggregation.<sup>141</sup> Generally, transition-metal disulfides with polar and sulfiphilic surfaces can effectively adsorb the generated dissolved polysulfides, leading to more satisfied cycle performances. While serving as sulfur hosts, they have some advantages working over their oxides counterparts: first, the metal-sulfur ionic bonds are accordingly weaker than metal-oxygen bonds, which makes them very competitive in electrocatalysis toward redox reaction in sulfur chemistry. And then, the electrical conductivity of metal sulfides is generally better than its oxides counterparts due to the softer bass of S<sup>2-</sup> than O<sup>2-</sup>, resulting in the weakness of the ionic nature and the reduction of the electron localization of metal-sulfur bonds. Consequently, the metal sulfides have lower lithiation voltage, which can avoid the failure of the sulfur hosts during charge/discharge cycles together with the strong sulfiphilic property for polysulfides inhibition.

## 12 | METAL NITRIDES

Owing to the fast electronic transferability as well as excellent physiochemical stability even under challenging conditions, transitional metal nitrides are well suited for a variety of energy-related applications.<sup>142–149</sup> Particularly, both generalized gradient approximation and local density approximation analysis reveal their metallic behavior with no resolved band gap. While being sulfur host materials, they possess quite a few merits including (1) strong chemical adsorption for polysulfides to effectively inhibit the shuttle effect; (2) a high electrical conductivity to accelerate the electrochemical conversion of adsorbed sulfur species on the surface, and (3) enhanced catalytic effects for further performance promotion. In an earlier time, Simon Ng et al. introduced layered tungsten nitride (WN), molybdenum nitride (Mo<sub>2</sub>N), and vanadium nitride (VN) as sulfur scaffolds to explore their enhanced capability for capturing polysulfides.<sup>143</sup> Since then, numerous nanostructured nitrides as sulfur cathodes are well developed, resulting in significant improvements in cycle performance. Over more recent times, titanium nitrides (TiN) hold great interest to be implemented as sulfur anchoring sites which deliver a much stable cycling span.<sup>150–153</sup> Zhang group proposes a multifunctional titanium nitride separator to retard polysulfides dissolution, fabricated by a simple coating process (Figure 10A).<sup>153</sup> The systematic first-principles calculations verify S atoms in Li<sub>2</sub>S<sub>n</sub> are inclined to bond with Ti atoms on the surface, while the Li atoms tend to bond with the N atoms, which results in large binding energies of up to 4 eV. Regarding this rewarding benefit of titanium nitride, Wang lab prepares a new type of ultrathin carbon-wrapped



titanium nano mesh using a rationally designed nano-confinement topochemical conversion strategy (Figure 10B).<sup>152</sup> The ultrathin 2D geometry with well-distributed pores offers plentiful exposed active sites and rapid charge transfer, leading to an outstanding electrocatalytic performance in tackling the sluggish sulfur redox kinetics. Apart from titanium nitrides, vanadium nitrides are also commonly studied. For example, the Li group reports highly conductive porous vanadium nitride/graphene, which exhibits significant chemical anchoring for polysulfides while also accelerating the kinetics of the redox reaction (Figure 10C).<sup>146</sup> Following, Tu and coauthors design the porous carbon fibers/vanadium nitride arrays composite scaffold for sulfur storage, via a facile chemical etching united solvothermal-supercritical fluid method (Figure 10D).<sup>145</sup> On it, sulfur can be stored on the backbone, and the dual blocking effects of “physical block and chemical absorption” are thereby achieved. Besides, such an advanced 3D scaffold is also implied to fabricate  $\text{Co}_4\text{N}/\text{N}$ -doped carbon composites shown in Figure 10E.<sup>154</sup> This will not only decrease the loading amount of the catalyst to further

improve the energy density of the electrode but also provide a large surface area to realize the uniform adsorption of soluble high-order polysulfides and deposition of the final discharge products ( $\text{Li}_2\text{S}_2/\text{Li}_2\text{S}$ ). However, the synthesis process of 2D metal nitrides is not easy, and it always involves high-temperature treatment under an  $\text{NH}_3$  atmosphere; thus, the key issue relies on the development of a facile efficient preparation way.

### 13 | OTHERS (METAL PHOSPHIDES, CARBIDES, BORIDES, MXENES, METAL ORGANIC FRAMEWORK, etc.)

Other transitional metal compounds including metal phosphides, carbides, borides, Mxenes as well as 2D metal-organic framework provide another potential choice for polysulfides regulation. Metal phosphides proposed by electronegative phosphorus atoms are also widely studied as sulfur hosts showing desirable chemical polarity for polysulfides trapping.<sup>155–159</sup> With the

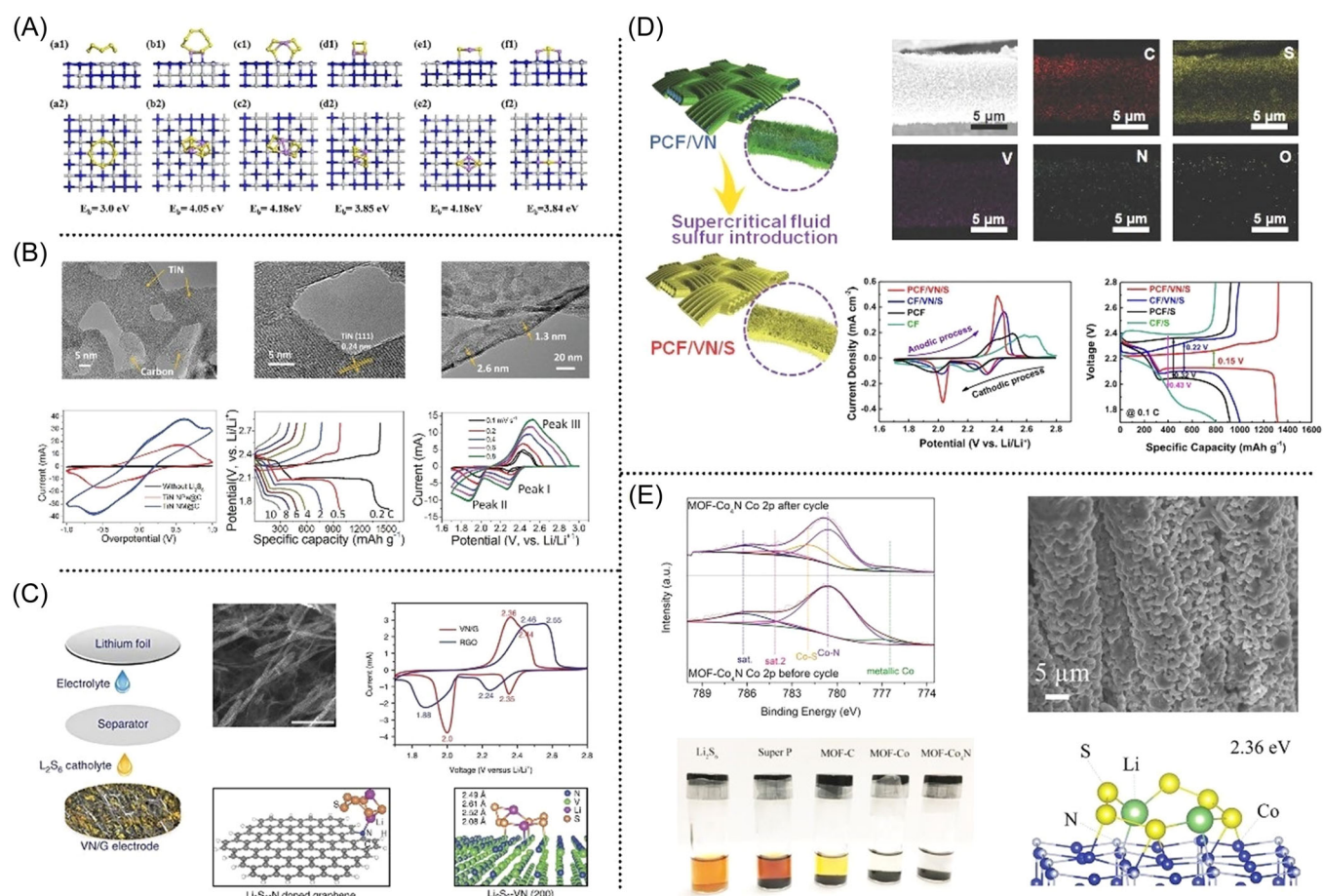
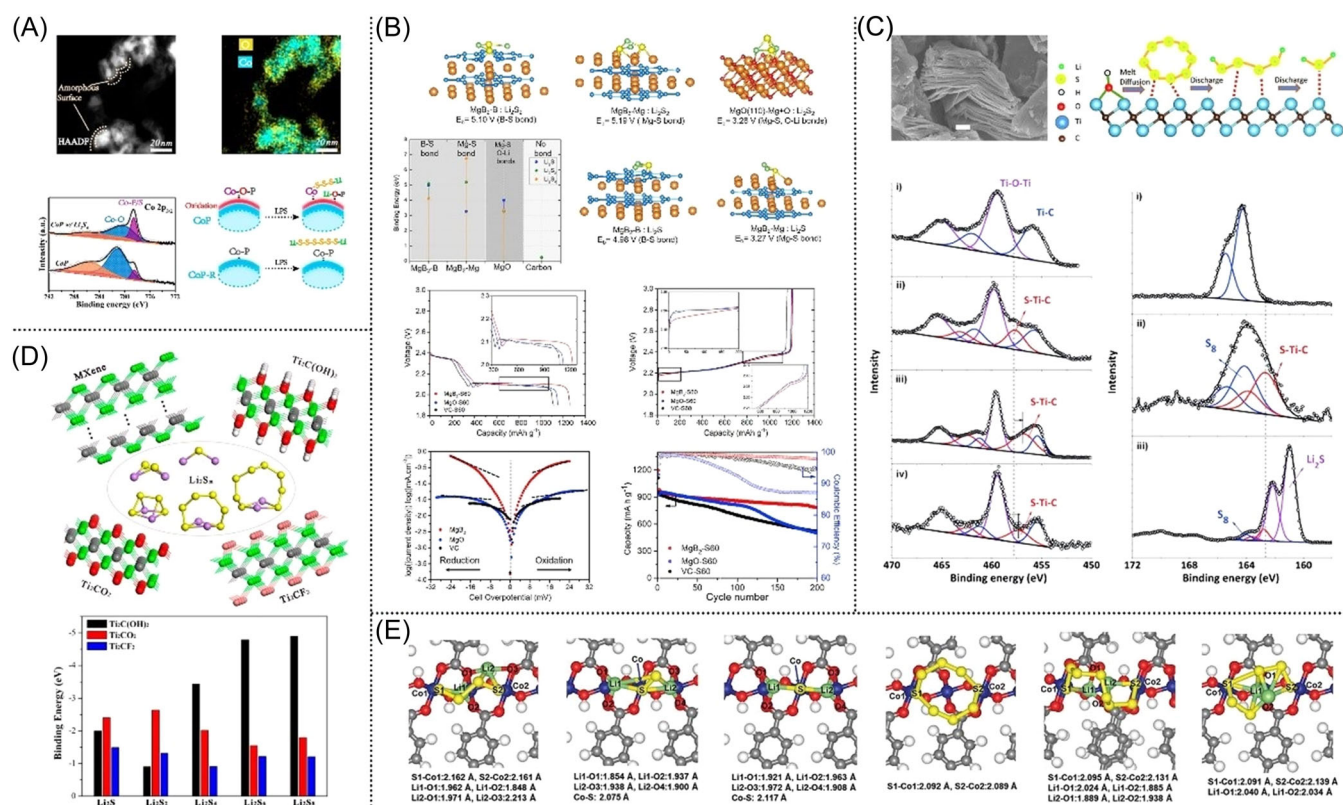


FIGURE 10 Metal nitrides: (A) TiN. Copyright 2019. *ChemistrySelect*; (B) TiN. Copyright 2021. *Small*; (C) VN. Copyright 2014. *Nat Comm*; (D) VN. Copyright 2018. *Adv Funct Mater*; (E) Co<sub>4</sub>N. Copyright 2021. *Small*.



appropriate atomic ratio of metal and P, transition metal phosphides endow a metallic character or even superconductivity.<sup>150,160–162</sup> Wang group claim for the first time that the active Co centrals derived from surface oxidation Co-O-P are the truly responsible sites for chemically binding with negatively charged S species (Figure 11A).<sup>155</sup> It has been identified that 3D transition metal oxides interact with sulfides via dominant oxygen–lithium binding while only minor metal–sulfur binding. By contrast, surface oxidation-activated binding mechanism unlocks the critical importance of stronger metal–sulfur binding, which is devoted to better-confining polysulfides and stabilizing cycling as well. Like the phosphides, metal borides such as Mg<sub>2</sub>B portrait high electron transfer and polysulfide immobilization capability. Nazar show by means of first-principles calculations that borides are unique in that both B- and Mg-terminated surfaces bond exclusively with the S<sub>x</sub><sup>2−</sup> anions (not Li<sup>+</sup>), and hence enhance electron transfer to the active S<sub>x</sub><sup>2−</sup> ions (Figure 11B).<sup>158</sup> 2D early-transition-metal carbides such as Ti<sub>2</sub>C also perform well as sulfur hosts owing to inherently metallic conductivity and self-functionalized surfaces. Nazar group demonstrated that the S-Ti-C bonding at the interface is responsible

for the strong interaction with polysulfide species (Figure 11C).<sup>163</sup> Ti<sub>2</sub>C delaminated from Ti<sub>2</sub>C(OH)<sub>x</sub> show excellent cycling stability at various rates over than Ti<sub>2</sub>C(OH)<sub>x</sub>. Generally, functionalized transitional metal carbides/nitrides constitute another important class of sulfur hosts, namely MXenes. It possesses the typical formula M<sub>n+1</sub>X<sub>n</sub>T<sub>x</sub> (n = 1–3), which is derived from the parental MAX phases by selectively etching the A layers (where M represents a transition metal, A represents the group 13 or 14 elements in the periodic table, X represents carbon or nitrogen, T<sub>x</sub> stands for the surface termination).<sup>164–166</sup> Owing to functional groups in surface terminations such as hydroxyl (–OH), oxygen (–O), chlorine (–Cl), and fluorine (–F), MXenes are also highly affinitive to polysulfides and can spontaneously attract them without additional surface modifications. Lu group systemically studies the interactions of lithium (poly)sulfides on Ti-based bare MXenes and surface functionalized Ti<sub>2</sub>C with –F, –O, and –OH groups by using density functional theory calculations.<sup>167</sup> It is found that the attractions of bare MXenes are strong enough to break the bonds of S–S and Li–S in lithium polysulfides, and thus strong Ti–S largely reduce the kinetics of sulfur, then influencing the performance of



**FIGURE 11** Metal phosphides/carbides/borides/Mxenes/metal-organic framework: (A) CoP. Copyright 2019 *J Am Chem Soc*; (B) MgB<sub>2</sub>. Copyright 2017 *Joule*; (C) TiC. Copyright 2019 *Agnew Chem*; (D) MXenes. Copyright 2018 *J Phys Chem C*; (E) MOF. Copyright 2020 *Adv Mater*.

batteries. By contrast, the intermediate (neither too weak nor too strong) interaction from functionalized  $\text{Ti}_2\text{C}$  would be the optimum. Compared with their oxide counterparts, transition metal phosphides/carbides/borides/MXenes present high electron transfer, which could largely reduce the additional carbon content employed to enhance its conductivity. Employing this technique, polysulfide loss is minimized, the surface redox chemistry is fast, and solid products are homogeneously deposited. Another indispensable case for sulfur loading is metal-organic framework, which naturally contains numerous chemically polar sites showing great potential for polysulfides regulation. Guo research group periodically arranges cobalt atoms coordinated with oxygen atoms via exposure on the surface of ultrathin MOF nanosheets, which serve as “traps” to suppress polysulfide shuttling by Lewis acid-base interaction.<sup>168</sup>

## 14 | COORDINATION ENGINEERING

It has been proved that the electrochemical performance differs from one host material to another, encompassing both metal-free and meal-based sulfur hosts and therefore illustrating distinct reaction kinetics over their surface.<sup>169–173</sup> Despite extensive research into the inner structure-property relationship, the essential principle for the rational sulfur cathode design has yet to be established due to the extremely complicated conversion process. Being a typical interfacial interaction, both anchoring and catalyzing effect are intrinsically governed by the cation and anion ligands from central active sites as well as locally surrounding atoms, which is further determined by their electronic redistribution.<sup>43</sup> As illustrated by the Qian group, diverse cobalt-based compounds  $\text{Co}_3\text{O}_4$ ,  $\text{CoS}_2$ ,  $\text{Co}_4\text{N}$ , and CoP with fixed metal cation and varied non-metal anions possess distinct chemical trapping capabilities toward polysulfides. Density functional theory calculation unravels unprecedented catalytic effect from CoP cathode is ascribed to the distinct upshift of p band centers with respect to Fermi level, thus enabling a reduced energy gap between Co 3d and P 2p centers. This higher hybridization in valence band electrons facilitates electron exchange, thereby promoting sulfides redox dynamics.<sup>43</sup> While using 2D materials as encapsulation materials for sulfur, there is a notable feature worth to be noted: quite a different chemical reactivity will be obtained from their terrace and edge sites due to the involved distinguished coordination structure from edge sites. Particularly, they are profiled as fascinating adsorption sites toward polysulfide prohibition. Besides, to greatly match rational binding energy, recently growing efforts have been given to coordination

regulation via defects engineering, dopants engineering, heterostructure engineering as well as lattice facet controlling so as to precisely tune the geometry chemistry and electronic structure of the center metal atoms.<sup>43,174</sup>

## 15 | EDGE-SITE EXPOSURE IN 2D STRUCTURE

Generally, the exposed facets, corners, steps, kinks, and edges on crystal surfaces have distinct electronic distribution compared with their bulk sites, resulting in varied chemical reactivity. It is anticipated that 2D materials with ultrathin layered structures may exhibit different chemical reactivity at edge sites composed of low-coordinated atoms and terrace locations out of fully coordinated atoms. One existing case illustrating different chemical reactivity between the terrace and edge sites is that the chemical electrodeposition preferentially takes place at the line edges of graphite, resulting in the formation of nanowires. Given this, it is highly anticipated that these disparities in physicochemical properties will have a considerable impact on the regulation of sulfur or sulfides. Cui group exploits well-defined edge-exposed (layer vertically aligned nanofilms) and terrace-exposed (horizontal nanosheets and nanocages)  $\text{MoS}_2$  samples to demonstrate high electrochemical selectivity of edge versus terrace sites for lithium sulfide ( $\text{Li}_2\text{S}$ ) electrochemical deposition (Figure 12A).<sup>133</sup> It has been shown that the edge sites of  $\text{MoS}_2$ , especially the unsaturated dangling-bond-enriched Mo-edge and S-edge, can interact with  $\text{Li}_2\text{S}$  more forcefully than their terrace equivalent. As a result, while utilized as a host material for sulfur loading, they exhibit both a high capacity for trapping polysulfides and a remarkable electrocatalytic activity for redox reactions. And then, Arava and co-authors successfully demonstrate the preferential adsorption of higher-order liquid polysulfides and subsequent conversion into lower-order solid species in the form of dendrite-like structures on the edge sites of  $\text{XS}_2$  ( $\text{X} = \text{W}, \text{Mo}$ ) nanosheets (Figure 12B).<sup>135</sup> Owing to their enriched catalytically active sites on edge locations, to date, many strategies devoted to enhanced adsorptive and catalytic effect are focusing on morphology control, including hollow microspheres and vertical arrangements, to expose more edge sites.

## 16 | DEFECTS ENGINEERING

The local coordination environment around central metals has resulted from the synergistic effects of both cationic and anionic ligands. Usually, the ordered

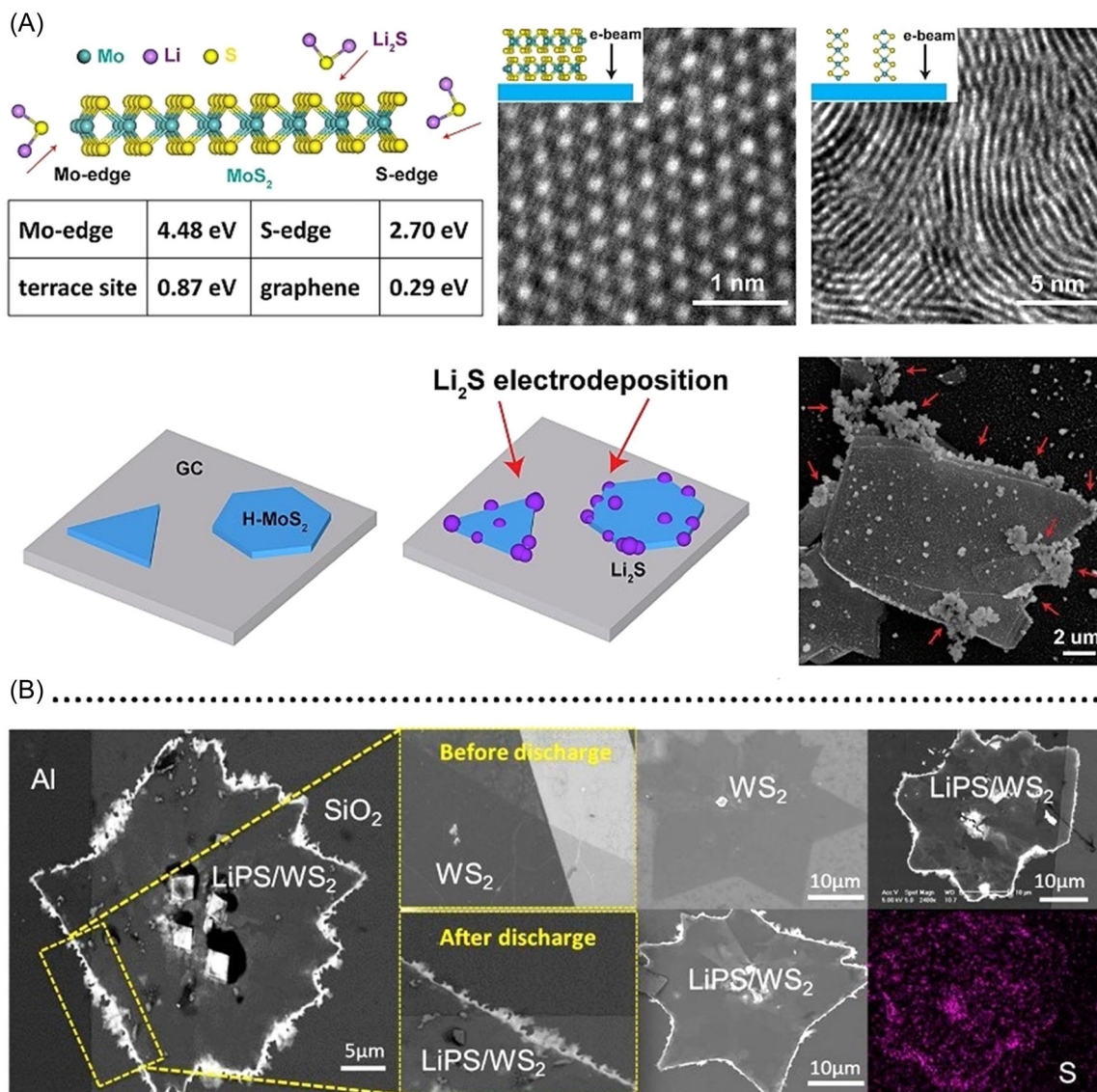


**FIGURE 12** Edge-sites exposure: (A) High electrochemical selectivity of edge versus terrace sites in MoS<sub>2</sub>. Copyright 2014. *Nano Lett*; (B) Preferential catalytic sites exploration of XS<sub>2</sub> (X = W, Mo). Copyright 2017. *J Am Chem Soc*.

crystalline planes of the host materials with a long-term range full of saturated electronic coordination are more likely to be chemically inert, which substantially restricts charge transfer and thereby limits their adsorptive-catalytic capability toward polysulfide molecules.<sup>92,175–177</sup> Typically, transitional metal compounds with rich anion defects, such as oxygen and sulfur vacancies, possess abundant dangling bonds acting as favorable electrocatalytic centers toward polysulfides regulation.<sup>177–179</sup> A recent study on anion vacancy exploration employs phosphorus vacancies-enriched CoP as the model to examine their significant role toward Li-S chemistry (Figure 13A).<sup>180</sup> As demonstrated, the derived phosphorus vacancies feature a low Co-P coordination number and accumulated electrons on Co

and P atoms, which therefore strengthen the chemical affinity to polysulfides and accelerate redox kinetics in Li-S chemistry. Another typical example can be seen in amorphous tantalum oxide with enriched oxygen vacancies (Figure 13B).<sup>181</sup> Currently, the amorphization strategy is regarded as an efficient way to realize defects-enriched 2D materials. XANES and EXAFS are employed to explore the close correlation of oxygen vacancy to enhanced catalytic capability. As demonstrated, an increased density of Ta 5d unoccupied states near the Fermi level is probably induced by the oxygen-vacancy defects, which implies defects enriched tantalum oxide possesses a lower CBM, desirable for electron transition. Generally, apart from the vacancy defects, “antisite” constitutes another class of points defects,



which provide an extra “regulating knob” in the optimization of carrier concentration to regulate the electrical conductivity, and hence affect the electrochemical performance.<sup>90</sup> Huang lab introduces high-density antisite defects in  $\text{Bi}_2\text{Te}_{2.7}\text{Se}_{0.3}$ , and utilize it to modify the separator and thus investigate its effect on Li-S battery. As identified, the antisite defects  $\text{Bi}'_{\text{Te}}$  coexist with Te vacancies  $\text{V}''_{\text{Te}}$ , while the former antisite sites are responsible for the enhanced adoptive-catalytic interaction toward polysulfides intermediates.

## 17 | DOPANTS ENGINEERING

Dopant engineering, which can adjust the electronic structures neighboring dopant atoms and thus affect the surface adsorption and catalytic process, has been recognized as a good strategy to solve the inherent issue in metal-sulfur chemistry.<sup>182–185</sup> Taking the anion N doping into  $\text{CoSe}_2$  for example, theoretical simulation analysis uncovers N doping that can result in a shorter Co-N bond with higher charge around Co centrals, thus creating new defects, and inducing the Co 3d band closer to the Fermi level. Further atomic-level analysis revealed that such optimized Co 3d orbits enable shorter Co-S bonds with absorbent sulfur/sulfides species, more efficiently weakening the S-S bridged bond of  $\text{Li}_2\text{S}_4$  and

Li-S bond of  $\text{Li}_2\text{S}$ , which eventually facilitates the polysulfide conversion reaction in the discharge process and the  $\text{Li}_2\text{S}$  oxidation in the charging process (Figure 14A).<sup>186</sup> More recently, an n-type degenerated semiconductor,  $\text{Bi}_2\text{Se}_3$ , is evaluated as a polysulfides modulator, on it, the covalently bonded quintuple atomic layers, Se-Bi-Se-Bi-Se, are held together by weak van der Waals interactions. Chou group uses a high-yield and scalable solution-based method to fabricate  $\text{Bi}_2\text{Se}_3$  nanosheets and further apply an iodine-doped way to vary its electronic distribution (Figure 14B).<sup>185</sup> It is revealed that the correlated blue-shift of the Bi 4f and Se 3d XPS spectra associated with an upward shift of the semiconductor Fermi level is realized via the doping role played by  $\text{I}^-$  ions at  $\text{Se}^{2-}$  sites, resulting in electronic redistribution as well as enhance conductivity. The  $\text{Li}_2\text{S}_4$  adsorption tests combined with DFT calculations demonstrate that the presence of I on the  $\text{Bi}_2\text{Se}_3$  surface further increases the absolute value of the binding energy, thus favoring polysulfides adsorption and hence potentially reducing the shuttle effect. Although more consolidated polysulfide adsorption and conversion have been obtained by introducing foreign dopant atoms, restricted by the existing means of characterization and detection at the atomic level; the underlying catalytic mechanism still lacks comprehensive understanding, which needs more experimental and theoretical investigation in the future.

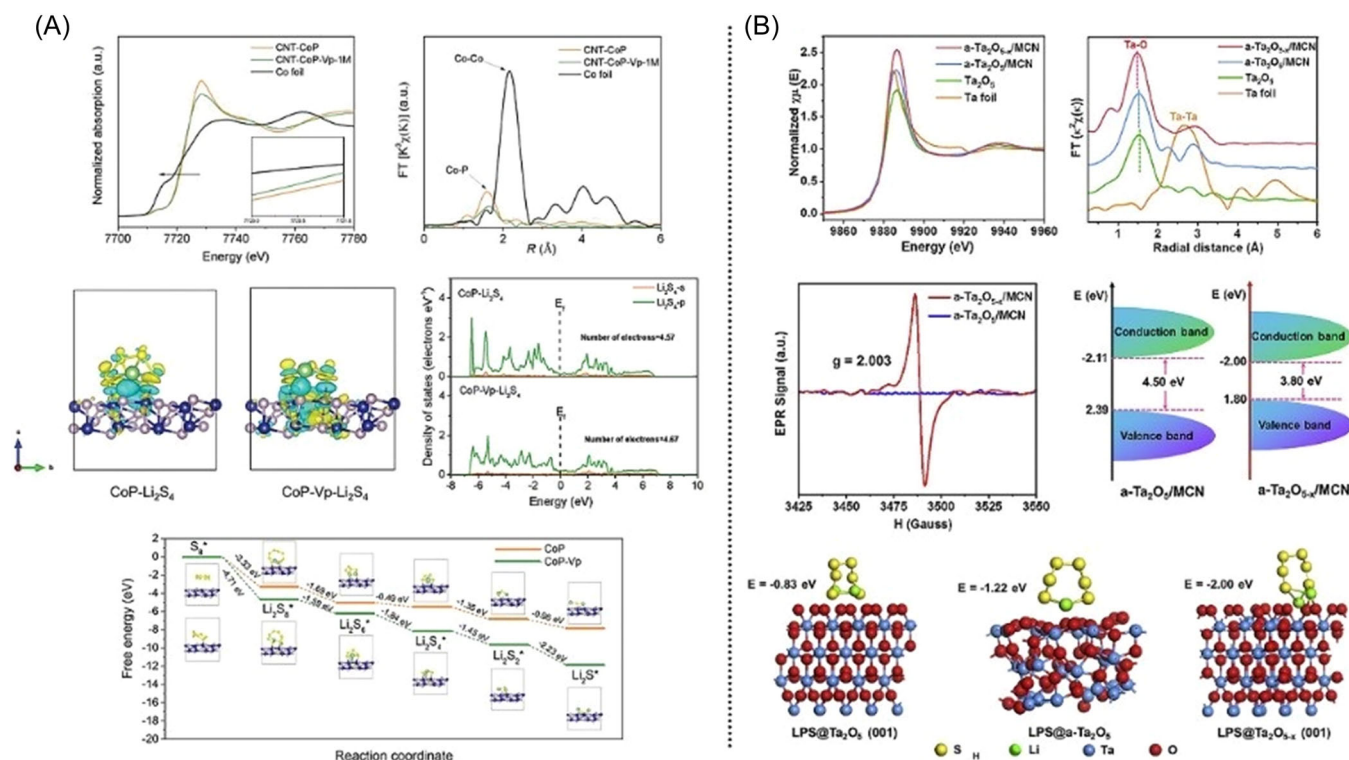


FIGURE 13 Defects engineering: (A) Phosphorus vacancies in cobalt phosphide. Copyright 2022. *Adv Energy Mater.* (B) Oxygen vacancies in tantalum oxide. Copyright 2022. *Matter.*



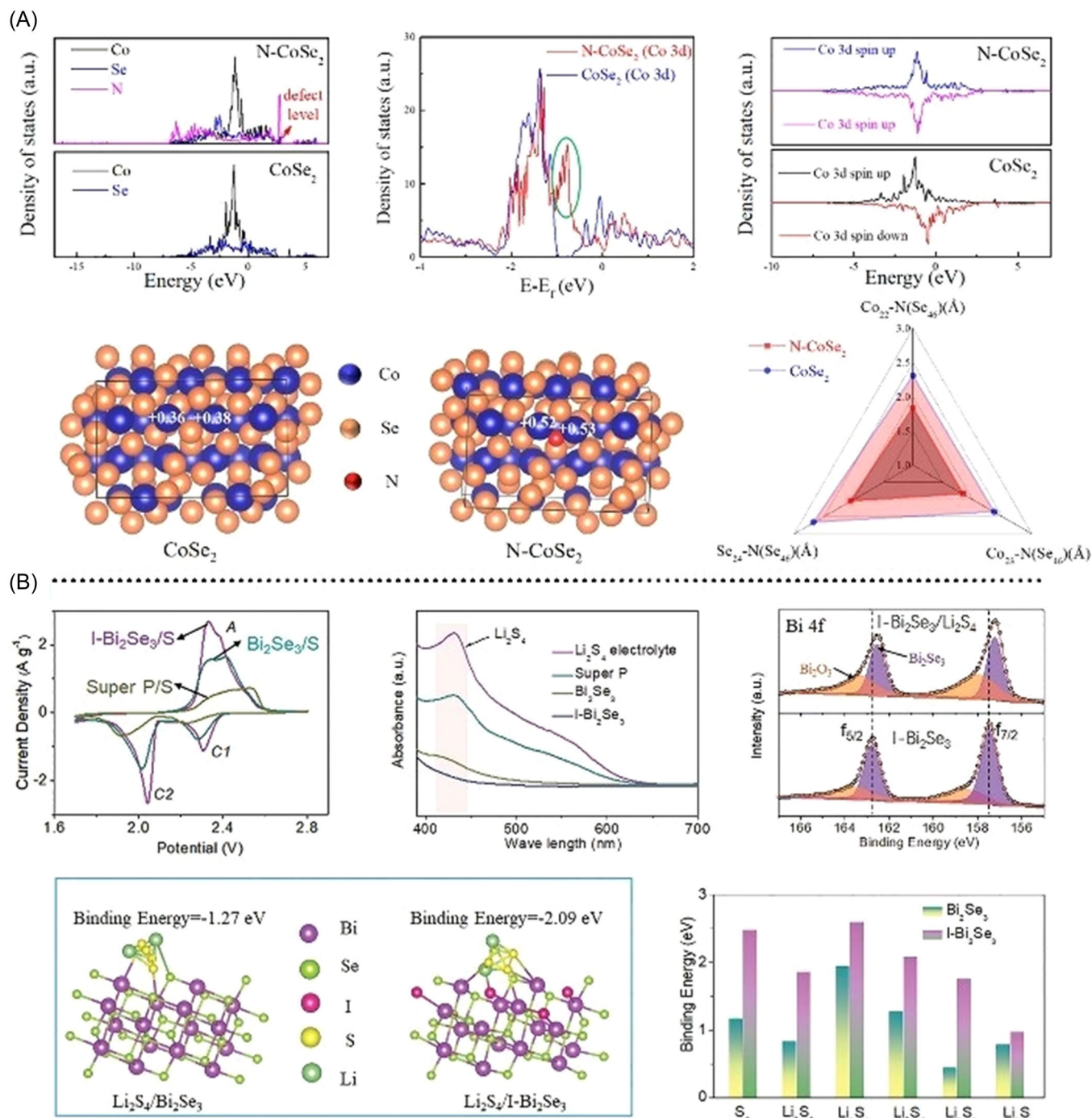
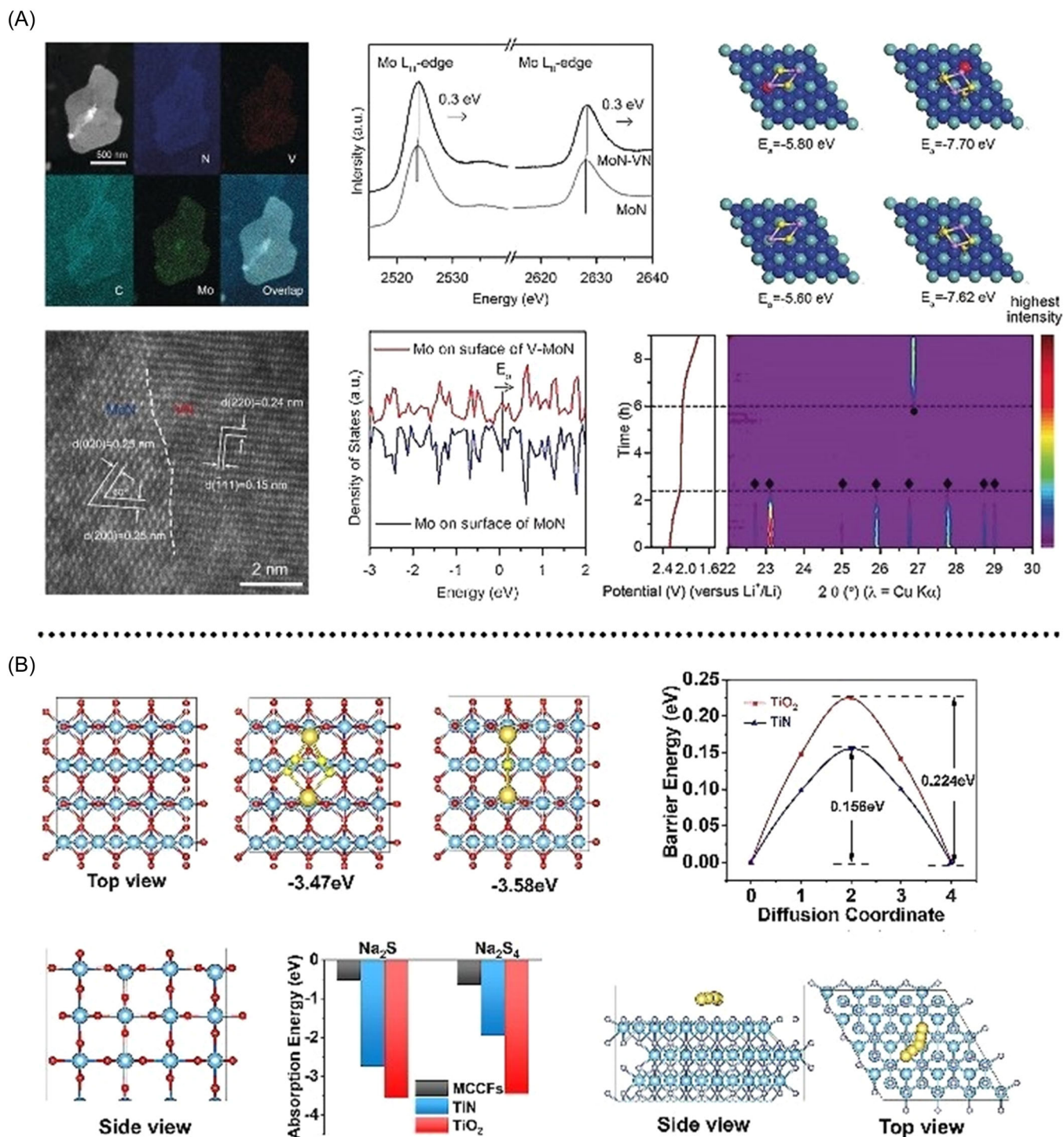


FIGURE 14 Dopants engineering: (A) Nitrogen-doped CoSe<sub>2</sub>. Copyright 2020. *ACS Energy Lett*; (B) Iodine-doped Bi<sub>2</sub>Se<sub>3</sub>. Copyright 2022. *Adv Func Mater*.

## 18 | HETEROSTRUCTURES ENGINEERING

Well, control in polysulfides may only be the final attempt if the reactive interface combines the merits of high electrical conductivity, high polysulfides adsorption, and high catalytic activity, and thus achieving smooth trapping–diffusion–conversion across this

desirable interface. Heterojunctions utilizing two or more components to vary the original physiochemical property have attracted increasing attention recently.<sup>187,188</sup> For example, 2D heterostructure MoN-VN is well designed as a typical model to gain an atom-level understanding of enhanced polysulfides adsorption over each constitute (Figure 15A).<sup>188</sup> NEXAFS data detect the shift on Mo LIII-edge and LII-edge spectrum



**FIGURE 15** Heterostructures engineering rewarding two respects: (A) Enhanced catalytic effects via introducing other components, for example, MoN-VN, Copyright 2018, *Angew Chem Int Ed*; (B) A combination of both enhanced adsorption capacity and electrical conversion ability via heterostructure engineering. Copyright 2021, *ACS Nano*.

to a higher energy location is closely associated with a reduced electron density of Mo central atoms, possibly due to stronger coupling between MoN and VN. Besides, as demonstrated by the theoretical calculations, induced V atoms tailor the electronic states of neighboring Mo atoms, thereby leading to better polysulfides adsorption

capability.<sup>188</sup> Besides, heterostructures can take into account the synergistic regulation of each ingredient, representing an ideal approach to realizing high-performance sulfur cathodes. In this regard, the twinborn TiO<sub>2</sub>-TiN heterostructure is delicately designed by Zheng and coauthors (Figure 15B).<sup>22</sup> On it, TiO<sub>2</sub> exhibits the

strongest adsorption capacity for different sulfur/sulfides species, while TiN has strong electrocatalytic ability enabling improved reaction kinetics. Therefore, the TiN-TiO<sub>2</sub> heterostructure combines the advantages of high adsorption capacity and strong electrical conversion ability, thus contributing a superior performance in charge and discharge processes. Heterostructures engineering suggests a reasonable orientation for sulfur host design, which is the combination of diverse advantages from each component and will greatly promote the practical use of Li-S batteries.

## 19 | PHASE ENGINEERING

Crystal facets, with distinct cation and anion ligands distribution, behave with varied adsorptive-catalytic effects toward polysulfide intermediates. Over the past, facets engineering to improve the absorption capacity and catalytic ability has aroused intensive interest. In earlier times, it has been reported that compared with graphene/2H MoS<sub>2</sub> heterostructure, the 1T phase heterostructure shows enhanced catalytic activity for polysulfides due to higher electronic conductivity, hydrophilic property, and denser active sites.<sup>189</sup> Later, Fan and coauthors compare 1T and 2H WS<sub>2</sub> functional separators in lithium-sulfur batteries combining theoretical calculations and experimental results. It is revealed that compared with 2H WS<sub>2</sub>, the metallic 1T phase exhibits much higher binding energy with sulfides species.<sup>190</sup> Besides, Zha et al. have shown TiO<sub>2</sub> with exposed (001) facet results in increased absorption ability as well as an accelerated redox reaction, which significantly enhances the cell performance (Figure 16A).<sup>191</sup> However, the desirable synthesis for nanomaterials with specific grain orientation structures remains challenging. Most recently, Luo and co-authors use 2D Ti<sub>3</sub>C<sub>2</sub> MXene as the initial raw nanomaterial to successfully fabricate (001) facet-dominated TiN nanoflakes (Figure 16B).<sup>151</sup> The prepared (001) facet-dominated TiN nanoflakes catalyze the conversion of soluble high-order polysulfides into Li<sub>2</sub>S<sub>2</sub>/Li<sub>2</sub>S to induce the Li<sub>2</sub>S uniform deposition in the discharge process and then decrease the delithiation barrier of Li<sub>2</sub>S in the charge process.<sup>180,181</sup>

## 20 | SUMMARY AND PERSPECTIVES

Polysulfides management including minimizing the shuttling effect and speeding up reaction kinetics is a long-term attempt toward a high-performance metal-sulfur battery. By far, a respectable performance could be realized through

integrating efforts from electrode material, separator as well as electrolyte. Regarding sulfur cathodes, several requirements should be preferably guaranteed: (1) higher electrical and ionic conductive channels to circumvent the insulating property of sulfur/sulfides family; (2) significant interface contacts along with enhanced absorptive-catalytic capability to mitigate shuttle effect and poor kinetics; (3) sufficient open space or adequate mechanical quality to account for sulfur volume change during charge-discharge, and so forth.

2D layered materials with easily adjustable morphology and physiochemistry show great promise to meet these requirements. From functionalized graphene and graphene analogs to diverse 2D metal/metal compounds and their hybrids, increasing attention is focusing on their interface chemistry devoted to enhanced adsorptive and catalytic effects. Functionalized carbon with a modified chemically polar interface out of functional groups or heteroatoms allows for more efficient polar-to-polar interaction with sulfur/sulfides species. On it, introducing functional groups onto graphene can not only increase the reactivity of aromatic carbon rings toward sulfur and sulfide species but also directly interact with them based on enhanced covalent binding. However, introducing functional groups onto the surface results in a destroyed C-C lattice, largely impeding electron/ion transfer. This, however, can be compensated by relocating heteroatoms (such as B, N, O, P, or S) into defective sites. Graphene analogs, including black phosphorus, carbon nitride, boron nitride, and so forth, representing another type of 2D metal-free host materials, also gain burgeoning concerns. The high concentration of electronegatively charged atoms along with asymmetric occupation causes asymmetric charge distribution, affecting the net polarity and thus creating active sites for binding polysulfides.

2D metal/metal compounds with Lewis acid centrals are highly suggested due to enhanced adsorption capability toward polysulfides. More importantly, most metal/metal mixtures show a rewarding capability to catalyze sulfur redox reactions by decreasing the conversion energy barrier. Such accelerated reaction kinetics is crucial to guarantee more reversible metal-sulfur chemistry. Especially at key steps, inadequate conversion of soluble long-chain sulfides into insoluble short-chain sulfides causes a concentration gradient and hence exacerbates the shutting effect and capacity loss. Being a typical interfacial interaction, both anchoring and catalyzing effect are intrinsically governed by the cation and anion ligands from central active sites as well as locally surrounding atoms, which is further determined by their electronic redistribution. Fine-tuning its composition via defect engineering,



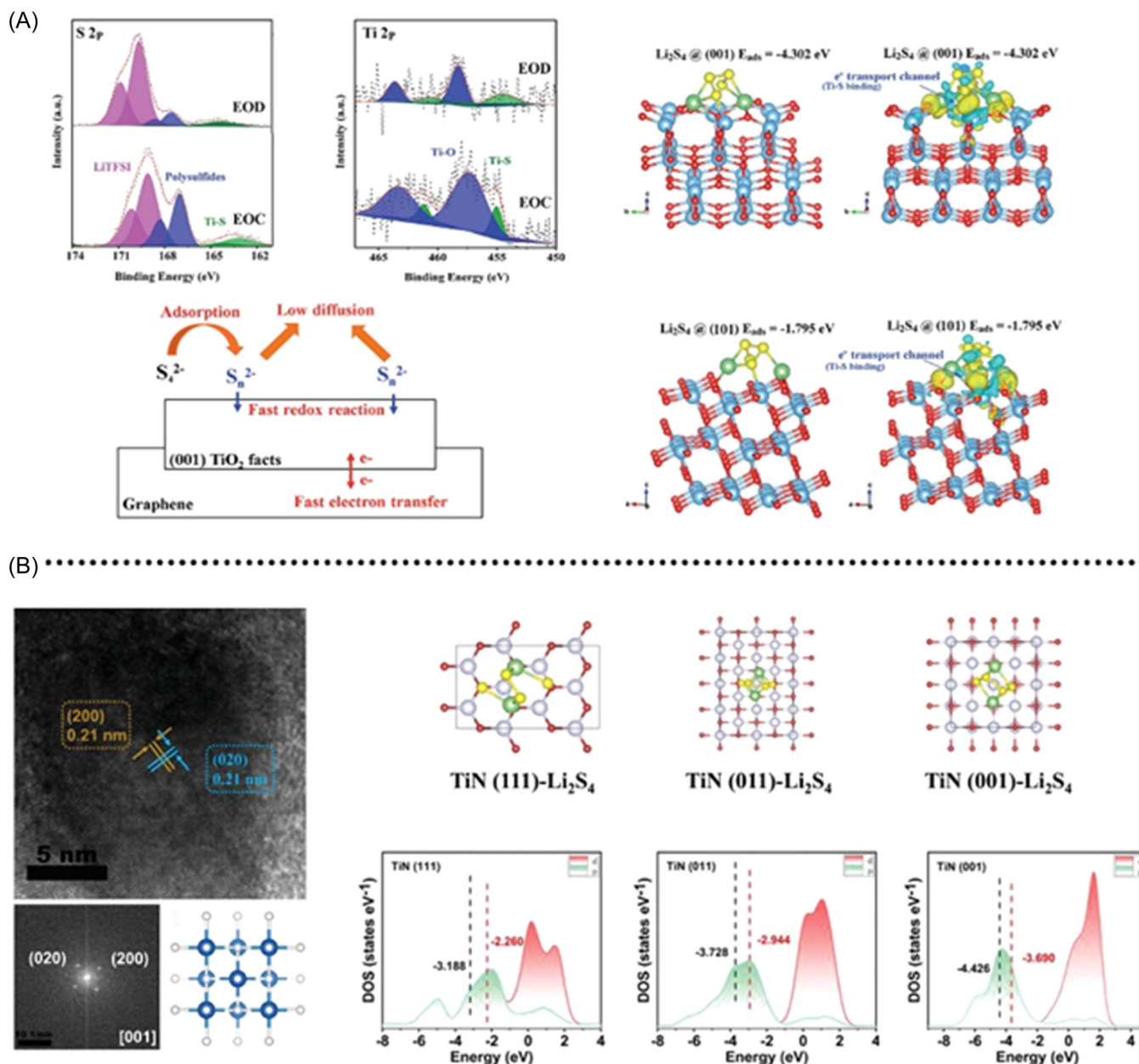


FIGURE 16 Phase engineering: (A) TiO<sub>2</sub> with exposed (001) facets. Copyright 2019. *J Mater Chem A*; (B) TiN with exposed (001) facets. Copyright 2021, *Small*.

heteroatom doping, heterostructure construction, phase control, and their hybridization is applied to vary electronic distribution and hence enhance chemical interaction with polysulfide intermediates.

Currently, despite extensive research into sulfur cathode design and their inner structure–property relationship, the essential principle for the rational sulfur cathode has yet to be established due to the extremely complicated conversion process. In the future, significant breakthroughs in mechanism exploration in Li-S chemistry are highly anticipated due to fast-increasing high-quality in situ characterization. Furthermore, the

advanced sulfur host can be realized via precise regulation from angstrom to the micron level.

## ACKNOWLEDGMENTS

The authors acknowledge the financial support from the Science and Technology Bureau of Huangpu District (2020GH03), the Innovation and Technology Fund-Partnership Research Programme (PRP/055/21FX), Innovation and Technology Fund-Guangdong Hong Kong Technology Cooperation Funding Scheme (GHP/047/20GD), Guangdong-Hong Kong-Macau Joint Laboratory for Photonic-Thermal-Electrical Energy Materials

and Devices (GDSTC No.2019B121205001), and Hong Kong Branch of National Precious Metals Material Engineering Research Center.

## CONFLICTS OF INTEREST STATEMENT

The authors declare no conflicts of interest.

## ORCID

Zijian Zheng  <https://orcid.org/0000-0002-6653-7594>

## REFERENCES

- Bruce PG, Freunberger SA, Hardwick LJ, Tarascon J-M. Li-O<sub>2</sub> and Li-S batteries with high energy storage. *Nat Mater*. 2012;11:19-29.
- Wei S, Xu S, Agrawal A, et al. A stable room-temperature sodium-sulfur battery. *Nat Commun*. 2016;7:11722.
- Ye C, Chao D, Shan J, Li H, Davey K, Qiao SZ. Unveiling the advances of 2D materials for Li/Na-S batteries experimentally and theoretically. *Matter*. 2020;2:323-344.
- Ding J, Zhang H, Fan W, Zhong C, Hu W, Mitlin D. Review of emerging potassium-sulfur batteries. *Adv Mater*. 2020;32:1908007.
- Ford HO, Doyle ES, He P, et al. Self-discharge of magnesium-sulfur batteries leads to active material loss and poor shelf life. *Energy Environ Sci*. 2021;14:890.
- Zhou D, Tang X, Zhang X, et al. Multi-ion strategy toward highly durable calcium/sodium-sulfur hybrid battery. *Nano Lett*. 2021;21:3548-3556.
- Pang Q, Liang X, Kwok CY, Nazar LF. Advances in lithium-sulfur batteries based on multifunctional cathodes and electrolytes. *Nat Energy*. 2016;1:16132.
- Chung SH, Manthiram A. Current status and future prospects of metal-sulfur batteries. *Adv Mater*. 2019;31:1901125.
- Manthiram A, Chung SH, Zu C. Lithium-sulfur batteries: progress and prospects. *Adv Mater*. 2015;27:1980-2006.
- Fang R, Zhao S, Sun Z, Wang DW, Cheng HM, Li F. More reliable lithium-sulfur batteries: status, solutions and prospects. *Adv Mater*. 2017;29:1606823.
- Gao Y, Guo Q, Zhang Q, Cui Y, Zheng Z. Fibrous materials for flexible Li-S battery. *Adv Energy Mater*. 2021;11:2002580.
- Zou Q, Lu YC. Liquid electrolyte design for metal-sulfur batteries: mechanistic understanding and perspective. *EcoMat*. 2021;3:e12115.
- Wu F, Chen S, Srot V, et al. A sulfur-limonene-based electrode for lithium-sulfur batteries: high-performance by self-protection. *Adv Mater*. 2018;30:1706643.
- Hu Y, Chen W, Lei T, et al. Strategies toward high-loading lithium-sulfur battery. *Adv Energy Mater*. 2020;10:2000082.
- Lin Z, Liu T, Ai X, Liang C. Aligning academia and industry for unified battery performance metrics. *Nat Commun*. 2018;9:5262.
- Fang R, Xu J, Wang DW. Covalent fixing of sulfur in metal-sulfur batteries. *Energy Environ Sci*. 2020;13:432.
- Fan H-N, Wang X-Y, Yu H-B, et al. Enhanced potassium ion battery by inducing interlayer anionic ligands in MoS<sub>1.5</sub>Se<sub>0.5</sub> nanosheets with exploration of the mechanism. *Adv Energy Mater*. 2020;10:1904162.
- Zhao X, Lu Y, Qian Z, Wang R, Guo Z. Potassium-sulfur batteries: status and perspectives. *EcoMat*. 2020;2:e12038.
- Lin D, Liu Y, Cui Y. Reviving the lithium metal anode for high-energy batteries. *Nat Nanotechnol*. 2017;12:194-206.
- Chen L, Yu H, Li W, Dirican M, Liu Y, Zhang X. Interlayer design based on carbon materials for lithium-sulfur batteries: a review. *J Mater Chem A*. 2020;8:10709-10735.
- Alzahrani AS, Otaki M, Wang D, et al. Confining sulfur in porous carbon by vapor deposition to achieve high-performance cathode for all-solid-state lithium-sulfur batteries. *ACS Energy Lett*. 2021;6:413-418.
- Fan L, Li M, Li X, Xiao W, Chen Z, Lu J. Interlayer material selection for lithium-sulfur batteries. *Joule*. 2019;3:361-386.
- Ye X, Ruan J, Pang Y, et al. Enabling a stable room-temperature sodium-sulfur battery cathode by building heterostructures in multichannel carbon fibers. *ACS Nano*. 2021;15:5639-5648.
- Tantis I, Bakandritsos A, Zaoralová D, et al. Covalently interlinked graphene sheets with sulfur-chains enable superior lithium-sulfur battery cathodes at full-mass level. *Adv Funct Mater*. 2021;31:2101326.
- Fang R, Zhao S, Pei S, et al. Toward more reliable lithium-sulfur batteries: an all-graphene cathode structure. *ACS Nano*. 2016;10:8676-8682.
- Peng H-J, Zhang Q. Designing host materials for sulfur cathodes: from physical confinement to surface chemistry. *Angew Chem Int Ed*. 2015;54:11018-11020.
- Fan H-N, Chen S-L, Chen X-H, et al. 3D selenium sulfide@carbon nanotube array as long-life and high-rate cathode material for lithium storage. *Adv Funct Mater*. 2018;28:1805018.
- Luo Y, Gao Y, Guo Q, Zheng Z. Interfacial design of thick sulfur cathodes to achieve high energy density and stability. *J Mater Chem A*. 2021;9:17129-17142.
- Yan Y, Zhang P, Qu Z, et al. Carbon/sulfur aerogel with adequate mesoporous channels as robust polysulfide confinement matrix for highly stable lithium-sulfur battery. *Nano Lett*. 2020;20:7662-7669.
- Razaq R, Zhang N, Xin Y, Li Q, Wang J, Zhang Z. Electrocatalytic conversion of lithium polysulfides by highly dispersed ultrafine Mo<sub>2</sub>C nanoparticles on hollow N-doped carbon flowers for Li-S batteries. *EcoMat*. 2020;2:e12020.
- Guo Y, Xu K, Wu C, Zhao J, Xie Y. Surface chemical-modification for engineering the intrinsic physical properties of inorganic two-dimensional nanomaterials. *Chem Soc Rev*. 2015;44:637-646.
- Jin H, Guo C, Liu X, et al. Emerging two-dimensional nanomaterials for electrocatalysis. *Chem Rev*. 2018;118:6337-6408.
- Ge Y, Shi Z, Tan C, et al. Two-dimensional nanomaterials with unconventional phases. *Chem*. 2020;6:1237-1253.
- Shao Q, Wu Z-S, Chen J. Two-dimensional materials for advanced Li-S batteries. *Energy Storage Mater*. 2019;22:284-310.
- Rojae R, Shahbazian-Yassar R. Two-dimensional materials to address the lithium battery challenges. *ACS Nano*. 2020;14:2628-2658.
- Yang T, Xia J, Piao Z, et al. Graphene-based materials for flexible lithium-sulfur batteries. *ACS Nano*. 2021;15:13901-13923.

37. Ji L, Rao M, Zheng H, et al. Graphene oxide as a sulfur immobilizer in high performance lithium/sulfur cells. *J Am Chem Soc.* 2011;133:18522-18525.
38. Zhou Y, Zhou C, Li Q, et al. Enabling prominent high-rate and cycle performances in one lithium-sulfur battery: designing permselective gateways for  $\text{Li}^+$  transportation in holey-CNT/S cathodes. *Adv Mater.* 2015;27:3774-3781.
39. Zhang J, Yang CP, Yin YX, Wan LJ, Guo YG. Sulfur encapsulated in graphitic carbon nanocages for high-rate and long-cycle lithium-sulfur batteries. *Adv Mater.* 2016;28:9539-9544.
40. He G, Evers S, Liang X, Cuisinier M, Garsuch A, Nazar LF. Tailoring porosity in carbon nanospheres for lithium-sulfur battery cathodes. *ACS Nano.* 2013;7:10920-10930.
41. Xiao X, Gao Y, Zhang L, et al. A promoted charge separation/transfer system from Cu single atoms and  $\text{C}_3\text{N}_4$  layers for efficient photocatalysis. *Adv Mater.* 2020;32:2003082.
42. Majdoub M, Anfar Z, Amedlous A. Emerging chemical functionalization of g- $\text{C}_3\text{N}_4$ : covalent/noncovalent modifications and applications. *ACS Nano.* 2020;14:12390-12469.
43. Zhou J, Liu X, Zhu L, et al. Deciphering the modulation essence of p bands in Co-based compounds on Li-S chemistry. *Joule.* 2018;2:2681-2693.
44. Aslam MK, Seymour ID, Katyal N, et al. Metal chalcogenide hollow polar bipyramid prisms as efficient sulfur hosts for Na-S batteries. *Nat Commun.* 2020;11:5242.
45. Li R, Rao D, Zhou J, et al. Amorphization-induced surface electronic states modulation of cobaltous oxide nanosheets for lithium-sulfur batteries. *Nat Commun.* 2021;12:3102.
46. Bhat A, Anwer S, Bhat KS, Mohideen MIH, Liao K, Qurashi A. Prospects challenges and stability of 2D MXenes for clean energy conversion and storage applications. *NPJ 2D Mater Appl.* 2021;5:61.
47. Al Salem H, Babu G, V. Rao C, Arava LMR. Electrocatalytic polysulfide traps for controlling redox shuttle process of Li-S batteries. *J Am Chem Soc.* 2015;137:11542-11545.
48. Li YJ, Fan JM, Zheng MS, Dong QF. A novel synergistic composite with multi-functional effects for high-performance Li-S batteries. *Energy Environ Sci.* 2016;9:1998.
49. Yu J, Xiao J, Li A, et al. Enhanced multiple anchoring and catalytic conversion of polysulfides by amorphous  $\text{MoS}_3$  nanoboxes for high-performance Li-S batteries. *Angew Chem Int Ed.* 2020;59:13071-13078.
50. Yang A, Zhou G, Kong X, et al. Electrochemical generation of liquid and solid sulfur on two-dimensional layered materials with distinct areal capacities. *Nat Nanotechnol.* 2020;15:231-237.
51. Yuan S, Guo Z, Wang L, Hu S, Wang Y, Xia Y. Leaf-like graphene-oxide-wrapped sulfur for high-performance lithium-sulfur battery. *Adv Sci.* 2015;2:1500071.
52. Wang C, Wang X, Yang Y, et al. Slurryless  $\text{Li}_2\text{S}$ /reduced graphene oxide cathode paper for high-performance lithium sulfur battery. *Nano Lett.* 2015;15:1796-1802.
53. Cao J, Chen C, Zhao Q, et al. A flexible nanostructured paper of a reduced graphene oxide-sulfur composite for high-performance lithium-sulfur batteries with unconventional configurations. *Adv Mater.* 2016;28:9629-9636.
54. Song J, Yu Z, Gordin ML, Wang D. Advanced sulfur cathode enabled by highly crumpled nitrogen-doped graphene sheets for high-energy-density lithium-sulfur batteries. *Nano Lett.* 2016;16:864-870.
55. Tan J, Li D, Liu Y, et al. A self-supported 3D aerogel network lithium-sulfur battery cathode: sulfur spheres wrapped with phosphorus doped graphene and bridged with carbon nanofibers. *J Mater Chem A.* 2020;8:7980-7990.
56. Handoko AD, Wei F, Yeo BS, Seh ZW. Understanding heterogeneous electrocatalytic carbon dioxide reduction through operando techniques. *Nat Catal.* 2018;1:922-934.
57. Liu X, Schlexer P, Xiao J, et al. pH effects on the electrochemical reduction of  $\text{CO}_2$  towards  $\text{C}_2$  products on stepped copper. *Nat Commun.* 2019;10:32.
58. Zhu Y, Wang J, Chu H, Chu YC, Chen HM. In situ/operando studies for designing next-generation electrocatalysts. *ACS Energy Lett.* 2020;5:1281-1291.
59. Xu H, Kong Z, Siegenthaler J, et al. Review on recent advances in two-dimensional nanomaterials-based cathodes for lithium-sulfur batteries. *EcoMat.* 2023;5:e12286.
60. Jiao L, Li H, Zhang C, et al. Molecular engineering of sulfur-providing materials for optimized sulfur conversion in Li-S chemistry. *EcoMat.* 2022;4:e12262.
61. Song Y, Gao H, Wang M, et al. Deciphering the defect micro-environment of graphene for highly efficient Li-S redox reactions. *EcoMat.* 2022;4:e12182.
62. Razaq R, Li P, Dong Y, Li Y, Mao Y, Bo SH. Practical energy densities, cost, and technical challenges for magnesium-sulfur batteries. *EcoMat.* 2020;2:e12056.
63. Zhang BW, Sheng T, Wang YX, et al. Long-life room-temperature sodium-sulfur batteries by virtue of transition-metal-nanocluster-sulfur interactions. *Angew Chem Int Ed.* 2019;58:1484-1488.
64. Liu J, Bao Z, Cui Y, et al. Pathways for practical high-energy long-cycling lithium metal batteries. *Nat Energy.* 2019;4:180-186.
65. Guo W, Zhang W, Si Y, Wang D, Fu Y, Manthiram A. Artificial dual solid-electrolyte interfaces based on in situ organothiol transformation in lithium sulfur battery. *Nat Commun.* 2021;12:3031.
66. Zeng FL, Zhou XY, Li N, et al. A multifunctional zipper-like sulfur electrode enables the stable operation of lithium-sulfur battery through self-healing chemistry. *Energy Storage Mater.* 2021;34:755-767.
67. Li D, Xie C, Gao Y, Hu H, Wang L, Zheng Z. Inverted anode structure for long-life lithium metal batteries. *Adv Energy Mater.* 2022;12:2200584.
68. Liu K, Zhang X, Miao F, et al. In situ electrochemical intercalation-induced phase transition to enhance catalytic performance for lithium-sulfur battery. *Small.* 2021;17:2100065.
69. Mu P, Dong T, Jiang H, et al. Crucial challenges and recent optimization progress of metal-sulfur battery electrolytes. *Energy Fuels.* 2021;35:1966.
70. Wang Y, Huang X, Zhang S, Hou Y. Sulfur hosts against the shuttle effect. *Small Methods.* 2018;2:1700345.
71. Wan H, Liu S, Deng T, et al. Bifunctional interphase-enabled  $\text{Li}_{10}\text{GeP}_2\text{S}_{12}$  electrolytes for lithium-sulfur battery. *ACS Energy Lett.* 2021;6:862-868.
72. Ji X, Lee KT, Nazar LF. A highly ordered nanostructured carbon-sulphur cathode for lithium-sulphur batteries. *Nat Mater.* 2009;8:500-506.



73. Bhargav A, He J, Gupta A, Manthiram A. Lithium-sulfur batteries: attaining the critical metrics. *Joule*. 2020;4:285-291.
74. Wang D, Chang J, Huang Q, et al. Crumpled, high-power, and safe wearable lithium-ion battery enabled by nanostructured metallic textiles. *Fundam Res*. 2021;1:399-407.
75. Seh ZW, Sun Y, Zhang Q, Cui Y. Designing high-energy lithium-sulfur batteries. *Chem Soc Rev*. 2016;45:5605-5634.
76. Huang L, Li J, Liu B, et al. Electrode design for lithium-sulfur batteries: problems and solutions. *Adv Funct Mater*. 2020;30:1910375.
77. Gorlin Y, Patel MUM, Freiberg A, et al. Understanding the charging mechanism of lithium-sulfur batteries using spatially resolved operando X-ray absorption spectroscopy. *J Electrochem Soc*. 2016;163:A930-A939.
78. Xu Z, Wang J, Yang J, et al. Enhanced performance of a lithium-sulfur battery using a carbonate-based electrolyte. *Angew Chem Int Ed*. 2016;55:10372-10375.
79. Ye C, Shan J, Chao D, et al. Catalytic oxidation of K<sub>2</sub>S via atomic Co and pyridinic N synergy in potassium-sulfur batteries. *J Am Chem Soc*. 2021;143:16902-16907.
80. Hua W, Li H, Pei C, et al. Selective catalysis remedies polysulfide shuttling in lithium-sulfur batteries. *Adv Mater*. 2021;33:2101006.
81. Pei F, Lin L, Ou D, et al. Self-supporting sulfur cathodes enabled by two-dimensional carbon yolk-shell nanosheets for high-energy-density lithium-sulfur batteries. *Nat Commun*. 2017;8:482.
82. Chen W, Lei T, Wu C, et al. Designing safe electrolyte systems for a high-stability lithium-sulfur battery. *Adv Energy Mater*. 2018;8:1702348.
83. Xu R, Cheng X-B, Yan C, et al. Artificial interphases for highly stable lithium metal anode. *Matter*. 2019;1:317-344.
84. Zhang S, Ueno K, Dokko K, Watanabe M. Recent advances in electrolytes for lithium-sulfur batteries. *Adv Energy Mater*. 2015;5:1500117.
85. Li X, Lushington A, Sun Q, et al. Safe and durable high-temperature lithium-sulfur batteries via molecular layer deposited coating. *Nano Lett*. 2016;16:3545-3549.
86. Wu F, Chu F, Ferrero GA, et al. Boosting high-performance in lithium-sulfur batteries via dilute electrolyte. *Nano Lett*. 2020;20:5391-5399.
87. Zhang B, Wu J, Gu J, Li S, Yan T, Gao XP. The fundamental understanding of lithium polysulfides in ether-based electrolyte for lithium-sulfur batteries. *ACS Energy Lett*. 2021;6:537-546.
88. Ren Y, Hortance N, McBride J, Hatzell KB. Sodium-sulfur batteries enabled by a protected inorganic/organic hybrid solid electrolyte. *ACS Energy Lett*. 2021;6:345-353.
89. Zou K, Li N, Dai X, et al. Lightweight freestanding CeF<sub>3</sub> nanorod/carbon nanotube composite interlayer for lithium-sulfur batteries. *ACS Appl Nano Mater*. 2020;3:5732-5742.
90. Li N, Yu L, Xi J. Integrated design of interlayer/current-collector: heteronanowires decorated carbon microtube fabric for high-loading and lean-electrolyte lithium-sulfur batteries. *Small*. 2021;17:2103001.
91. He D, Meng J, Chen X, et al. Ultrathin conductive interlayer with high-density antisite defects for advanced lithium-sulfur batteries. *Adv Funct Mater*. 2021;31:2001201.
92. Luo S, Ruan J, Wang Y, et al. Flower-like interlayer-expanded MoS<sub>2-x</sub> nanosheets confined in hollow carbon spheres with high-efficiency electrocatalysis sites for advanced sodium-sulfur battery. *Small*. 2021;17:2101879.
93. Gangatharan PM, Maubane-Nkadameng MS, Coville NJ. Building carbon structures inside hollow carbon spheres. *Sci Rep*. 2019;9:10642.
94. Zhao MQ, Liu XF, Zhang Q, et al. Graphene/single-walled carbon nanotube hybrids: one-step catalytic growth and applications for high-rate Li-S batteries. *ACS Nano*. 2012;6:10759-10769.
95. Zhou W, Wang C, Zhang Q, et al. Tailoring pore size of nitrogen-doped hollow carbon nanospheres for confining sulfur in lithium-sulfur batteries. *Adv Energy Mater*. 2015;5:1401752.
96. Gueon D, Hwang JT, Yang SB, et al. Spherical macroporous carbon nanotube particles with ultrahigh sulfur loading for lithium-sulfur battery cathodes. *ACS Nano*. 2018;12:226-233.
97. Du Z, Chen X, Hu W, et al. Cobalt in nitrogen-doped graphene as single-atom catalyst for high-sulfur content lithium-sulfur batteries. *J Am Chem Soc*. 2019;141:3977-3985.
98. Chen H, Zhou G, Boyle D, et al. Electrode design with integration of high tortuosity and sulfur-philicity for high-performance lithium-sulfur battery. *Matter*. 2020;2:1605-1620.
99. Zheng X, Li P, Dou S, et al. Non-carbon-supported single-atom site catalysts for electrocatalysis. *Energy Environ Sci*. 2021;14:2809.
100. Chen J, Wang L. Effects of the catalyst dynamic changes and influence of the reaction environment on the performance of electrochemical CO<sub>2</sub> reduction. *Adv Mater*. 2022;34:2103900.
101. Lu Y, Liu T, Dong C-L, et al. Tailoring competitive adsorption sites by oxygen-vacancy on cobalt oxides to enhance the electrooxidation of biomass. *Adv Mater*. 2022;34:2107185.
102. Zhou G, Yin LC, Wang DW, et al. Fibrous hybrid of graphene and sulfur nanocrystals for high-performance lithium-sulfur batteries. *ACS Nano*. 2013;7:5367-5375.
103. Wang Z, Dong Y, Li H, et al. Enhancing lithium-sulphur battery performance by strongly binding the discharge products on amino-functionalized reduced graphene oxide. *Nat Commun*. 2014;5:5002.
104. Zhou L, Lin X, Huang T, Yu A. Binder-free phenyl sulfonated graphene/sulfur electrodes with excellent cyclability for lithium sulfur batteries. *J Mater Chem A*. 2014;2:5117.
105. Seh ZW, Wang H, Hsu P-C, et al. Facile synthesis of Li<sub>2</sub>S-polypyrrole composite structures for high-performance Li<sub>2</sub>S cathodes. *Energy Environ Sci*. 2014;7:672.
106. Qiu Y, Li W, Zhao W, et al. High-rate, ultralong cycle-life lithium/sulfur batteries enabled by nitrogen-doped graphene. *Nano Lett*. 2014;14:4821-4827.
107. Pang Q, Tang J, Huang H, et al. A nitrogen and sulfur dual-doped carbon derived from polyrhodanine@cellulose for advanced lithium-sulfur batteries. *Adv Mater*. 2015;27:6021-6028.
108. Zhou G, Paek E, Hwang GS, Manthiram A. Long-life Li/polysulphide batteries with high sulphur loading enabled by

- lightweight three-dimensional nitrogen/sulphur-codoped graphene sponge. *Nat Commun.* 2015;6:7760.
109. Hou TZ, Chen X, Peng H-J, et al. Design principles for heteroatom-doped nanocarbon to achieve strong anchoring of polysulfides for lithium-sulfur batteries. *Small.* 2016;12:3283-3291.
  110. Wang J, Han WQ. A review of heteroatom doped materials for advanced lithium-sulfur batteries. *Adv Funct Mater.* 2022;32:2107166.
  111. Tang C, Zhang Q, Zhao MQ, et al. Nitrogen-doped aligned carbon nanotube/graphene sandwiches: facile catalytic growth on bifunctional natural catalysts and their applications as scaffolds for high-rate lithium-sulfur batteries. *Adv Mater.* 2014;26:6100-6105.
  112. Song J, Xu T, Gordin ML, et al. Nitrogen-doped mesoporous carbon promoted chemical adsorption of sulfur and fabrication of high-area-capacity sulfur cathode with exceptional cycling stability for lithium-sulfur batteries. *Adv Funct Mater.* 2014;24:1243-1250.
  113. Yuan S, Bao JL, Wang L, Xia Y, Truhlar DG, Wang Y. Graphene-supported nitrogen and boron rich carbon layer for improved performance of lithium-sulfur batteries due to enhanced chemisorption of lithium polysulfides. *Adv Energy Mater.* 2016;6:1501733.
  114. Hou TZ, Xu WT, Chen X, Peng HJ, Huang JQ, Zhang Q. Lithium bond chemistry in lithium-sulfur batteries. *Angew Chem Int Ed.* 2017;56:8178-8182.
  115. Fan Y, Yang Z, Hua W, et al. Functionalized boron nitride nanosheets/graphene interlayer for fast and long-life lithium-sulfur batteries. *Adv Energy Mater.* 2017;7:1602380.
  116. Li L, Chen L, Mukherjee S, et al. Phosphorene as a polysulfide immobilizer and catalyst in high-performance lithium-sulfur batteries. *Adv Mater.* 2017;29:1602734.
  117. Deng DR, Xue F, Bai CD, et al. Enhanced adsorptions to polysulfides on graphene-supported BN nanosheets with excellent Li-S battery performance in a wide temperature range. *ACS Nano.* 2018;12:11120-11129.
  118. Xu ZL, Lin S, Onofrio N, et al. Exceptional catalytic effects of black phosphorus quantum dots in shuttling-free lithium sulfur batteries. *Nat Commun.* 2018;9:4164.
  119. Sun J, Sun Y, Pasta M, et al. Entrapment of polysulfides by a black-phosphorus-modified separator for lithium-sulfur batteries. *Adv Mater.* 2016;28:9797-9803.
  120. Zhang J, Li JY, Wang WP, et al. Microemulsion assisted assembly of 3D porous s/graphene@g-C<sub>3</sub>N<sub>4</sub> hybrid sponge as free-standing cathodes for high energy density Li-S batteries. *Adv Energy Mater.* 2018;8:1702839.
  121. Wang L, Chen W, Zhang D, et al. Surface strategies for catalytic CO<sub>2</sub> reduction: from two-dimensional materials to nanoclusters to single atoms. *Chem Soc Rev.* 2019;48:5310-5349.
  122. Shi Q, Zhu C, Du D, Lin Y. Robust noble metal-based electrocatalysts for oxygen evolution reaction. *Chem Soc Rev.* 2019;48:3181-3192.
  123. Zhou L, Martinez JMP, Finzel J, et al. Light-driven methane dry reforming with single atomic site antenna-reactor plasmonic photocatalysts. *Nat Energy.* 2020;5:61-70.
  124. Ng SF, Lau MYL, Ong WJ. Lithium-sulfur battery cathode design: tailoring metal-based nanostructures for robust polysulfide adsorption and catalytic conversion. *Adv Mater.* 2021;33:2008654.
  125. Li J, Niu Z, Guo C, Li M, Bao W. Catalyzing the polysulfide conversion for promoting lithium sulfur battery performances: a review. *J Energy Chem.* 2021;54:434-451.
  126. Wang N, Wang Y, Bai Z, et al. High-performance room-temperature sodium-sulfur battery enabled by electrocatalytic sodium polysulfides full conversion. *Energy Environ Sci.* 2020;13:562.
  127. Liu Z, Zhou L, Ge Q, et al. Atomic iron catalysis of polysulfide conversion in lithium-sulfur batteries. *ACS Appl Mater Interfaces.* 2018;10:19311-19317.
  128. Liang X, Hart C, Pang Q, Garsuch A, Weiss T, Nazar LF. A highly efficient polysulfide mediator for lithium-sulfur batteries. *Nat Commun.* 2015;6:5682.
  129. Tao X, Wang J, Liu C, et al. Balancing surface adsorption and diffusion of lithium-polysulfides on nonconductive oxides for lithium-sulfur battery design. *Nat Commun.* 2016;7:11203.
  130. Qiu W, Li G, Luo D, et al. Hierarchical micro-nanoclusters of bimetallic layered hydroxide polyhedrons as advanced sulfur reservoir for high-performance lithium-sulfur batteries. *Adv Sci.* 2021;8:2003400.
  131. Zhang Y, Liu X, Wu L, et al. A flexible, hierarchically porous PANI/MnO<sub>2</sub> network with fast channels and an extraordinary chemical process for stable fast-charging lithium-sulfur batteries. *J Mater Chem A.* 2020;8:2741-2751.
  132. Faber MS, Dziedzic R, Lukowski MA, Kaiser NS, Ding Q, Jin S. High-performance electrocatalysis using metallic cobalt pyrite (CoS<sub>2</sub>) micro- and nanostructures. *J Am Chem Soc.* 2014;136:10053-10061.
  133. Park J, Yu BC, Park JS, et al. Tungsten disulfide catalysts supported on a carbon cloth interlayer for high performance Li-S battery. *Adv Energy Mater.* 2017;7:1602567.
  134. Pu J, Shen Z, Zheng J, et al. Multifunctional Co<sub>3</sub>S<sub>4</sub>@sulfur nanotubes for enhanced lithium-sulfur battery performance. *Nano Energy.* 2017;37:7-14.
  135. Wang H, Zhang Q, Yao H, et al. High electrochemical selectivity of edge versus terrace sites in two-dimensional layered MoS<sub>2</sub> materials. *Nano Lett.* 2014;14:7138-7144.
  136. Yuan Z, Peng HJ, Hou TZ, et al. Powering lithium-sulfur battery performance by propelling polysulfide redox at sulfiphilic hosts. *Nano Lett.* 2016;16:519-527.
  137. Babu G, Masurkar N, Al Salem H, Arava LMR. Transition metal dichalcogenide atomic layers for lithium polysulfides electrocatalysis. *J Am Chem Soc.* 2017;139:171-178.
  138. Pang Q, Kundu D, Nazar LF. A graphene-like metallic cathode host for long-life and high-loading lithium-sulfur batteries. *Mater Horiz.* 2016;3:130-136.
  139. Xu J, Yang L, Cao S, et al. Sandwiched cathodes assembled from CoS<sub>2</sub>-modified carbon clothes for high-performance lithium-sulfur batteries. *Adv Sci.* 2021;8:2101019.
  140. Cheng Z, Chen Y, Yang Y, et al. Metallic MoS<sub>2</sub> nanoflowers decorated graphene nanosheet catalytically boosts the volumetric capacity and cycle life of lithium-sulfur batteries. *Adv Energy Mater.* 2021;11:2003718.
  141. Huang X, Tang J, Luo B, et al. Sandwich-like ultrathin TiS<sub>2</sub> nanosheets confined within N, S codoped porous carbon as an effective polysulfide promoter in lithium-sulfur batteries. *Adv Energy Mater.* 2019;9:1901872.

142. Balogun MS, Huang Y, Qiu W, Yang H, Ji H, Tong Y. Updates on the development of nanostructured transition metal nitrides for electrochemical energy storage and water splitting. *Mater Today*. 2017;20:425-451.
143. Huang ZD, Fang Y, Yang M, et al. Sulfur in mesoporous tungsten nitride foam blocks: a rational lithium polysulfide confinement experimental design strategy augmented by theoretical predictions. *ACS Appl Mater Interfaces*. 2019;11:20013-20021.
144. Hao Z, Yuan L, Chen C, et al. TiN as a simple and efficient polysulfide immobilizer for lithium-sulfur batteries. *J Mater Chem A*. 2016;4:17711-17717.
145. Shen Z, Zhang Z, Li M, et al. Rational design of a  $\text{Ni}_3\text{N}_{0.85}$  electrocatalyst to accelerate polysulfide conversion in lithium-sulfur batteries. *ACS Nano*. 2020;14:6673-6682.
146. Ma F, Srinivas K, Zhang X, et al.  $\text{Mo}_2\text{N}$  quantum dots decorated N-doped graphene nanosheets as dual-functional interlayer for dendrite-free and shuttle-free lithium-sulfur batteries. *Adv Funct Mater*. 2022;32:2206113.
147. Mosavati N, Salley SO, Ng KYS. Characterization and electrochemical activities of nanostructured transition metal nitrides as cathode materials for lithium sulfur batteries. *J Power Sources*. 2017;340:210-216.
148. Zhong Y, Chao D, Deng S, et al. Confining sulfur in integrated composite scaffold with highly porous carbon fibers/vanadium nitride arrays for high-performance lithium-sulfur batteries. *Adv Funct Mater*. 2018;28:1706391.
149. Sun Z, Zhang J, Yin L, et al. Conductive porous vanadium nitride/graphene composite as chemical anchor of polysulfides for lithium-sulfur batteries. *Nat Commun*. 2017;8:14627.
150. Cui Z, Zu C, Zhou W, Manthiram A, Goodenough JB. Mesoporous titanium nitride-enabled highly stable lithium-sulfur batteries. *Adv Mater*. 2016;28:6926-6931.
151. Peng T, Zhang N, Yang Y, et al. Crystal facet engineering of MXene-derived TiN nanoflakes as efficient bidirectional electrocatalyst for advanced lithium-sulfur batteries. *Small*. 2022;18:2202917.
152. Huang X, Tang J, Qiu T, et al. Nanoconfined topochemical conversion from MXene to ultrathin non-layered TiN nanomesh toward superior electrocatalysts for lithium-sulfur batteries. *Small*. 2021;17:2101360.
153. Xu G, Yan Q, Bai P, Dou H, Nie P, Zhang X. Nano-sized titanium nitride functionalized separator improves cycling performance of lithium sulfur batteries. *ChemistrySelect*. 2019;4:698-704.
154. Xiao K, Wang J, Chen Z, et al. Improving polysulfides adsorption and redox kinetics by the  $\text{Co}_4\text{N}$  nanoparticle/N-doped carbon composites for lithium-sulfur batteries. *Small*. 2019;15:1901454.
155. Zhong Y, Yin L, He P, Liu W, Wu Z, Wang H. Surface chemistry in cobalt phosphide-stabilized lithium-sulfur batteries. *J Am Chem Soc*. 2018;140:1455-1459.
156. Mi Y, Liu W, Li X, Zhuang J, Zhou H, Wang H. High-performance Li-S battery cathode with catalyst-like carbon nanotube-MoP promoting polysulfide redox. *Nano Res*. 2017;10:3698-3705.
157. Pang Q, Kundu D, Cuisinier M, Nazar LF. Surface-enhanced redox chemistry of polysulfides on a metallic and polar host for lithium-sulphur batteries. *Nat Commun*. 2014;5:4759.
158. Peng HJ, Zhang G, Chen X, et al. Enhanced electrochemical kinetics on conductive polar mediators for lithium-sulfur batteries. *Angew Chem Int Ed*. 2016;55:12990-12995.
159. Pang Q, Kwok CY, Kundu D, Liang X, Nazar LF. Lightweight metallic  $\text{MgB}_2$  mediates polysulfide redox and promises high-energy-density lithium-sulfur batteries. *Joule*. 2019;3:136-148.
160. Deng DR, Xue F, Jia YJ, et al.  $\text{Co}_4\text{N}$  nanosheet assembled mesoporous sphere as a matrix for ultrahigh sulfur content lithium-sulfur batteries. *ACS Nano*. 2017;11:6031-6039.
161. Zhou T, Lv W, Li J, et al. Twinborn  $\text{TiO}_2$ -TiN heterostructures enabling smooth trapping-diffusion-conversion of polysulfides towards ultralong life lithium-sulfur batteries. *Energy Environ Sci*. 2017;10:1694.
162. Wang J, Zhao Y, Li G, et al. Aligned sulfur-deficient  $\text{ZnS}_{1-x}$  nanotube arrays as efficient catalyzer for high-performance lithium/sulfur batteries. *Nano Energy*. 2021;84:105891.
163. Liang X, Garsuch A, Nazar LF. Sulfur cathodes based on conductive MXene nanosheets for high-performance lithium-sulfur batteries. *Angew Chem Int Ed*. 2015;54:3907-3911.
164. Zhang C, Cui L, Abdolhosseinzadeh S, Heier J. Two-dimensional MXenes for lithium-sulfur batteries. *InfoMat*. 2020;2:613-638.
165. Giebler L, Balach J. MXenes in lithium-sulfur batteries: scratching the surface of a complex 2D material-a minireview. *Mater Today Commun*. 2021;27:102323.
166. Wang Y, Guo T, Alhajji E, et al. MXenes for sulfur-based batteries. *Adv Energy Mater*. 2023;13:2202860.
167. Rao D, Zhang L, Wang Y, et al. Mechanism on the improved performance of lithium sulfur batteries with MXene-based additives. *The Journal of Physical Chemistry C*. 2017;121:11047-11054.
168. Li Y, Lin S, Wang D, et al. Single atom array mimic on ultrathin MOF nanosheets boosts the safety and life of lithium-sulfur batteries. *Adv Mater*. 2020;32:1906722.
169. Cheng M, Yan R, Yang Z, et al. Polysulfide catalytic materials for fast-kinetic metal-sulfur batteries: principles and active centers. *Adv Sci*. 2022;9:2102217.
170. Yang Y, Yang H, Wang X, Bai Y, Wu C. Multivalent metal-sulfur batteries for green and cost-effective energy storage: current status and challenges. *J Energy Chem*. 2022;64:144-165.
171. Ye H, Li Y. Room-temperature metal-sulfur batteries: what can we learn from lithium-sulfur. *InfoMat*. 2022;4:e12291.
172. Hao H, Wang Y, Katyal N, et al. Molybdenum carbide electrocatalyst in situ embedded in porous nitrogen-rich carbon nanotubes promotes rapid kinetics in sodium-metal-sulfur batteries. *Adv Mater*. 2022;34:2106572.
173. Wang R, Li M, Zhang Y, Sun K, Bao W. Atomic surface modification strategy of MXene materials for high-performance metal sulfur batteries. *Int J Energy Res*. 2022;46:11659-11675.
174. Zhang L, Liu D, Muhammad Z, et al. Single nickel atoms on nitrogen-doped graphene enabling enhanced kinetics of lithium-sulfur batteries. *Adv Mater*. 2019;31:1903955.
175. Wang X, Zhang Y, Si H, et al. Single-atom vacancy defect to trigger high-efficiency hydrogen evolution of  $\text{MoS}_2$ . *J Am Chem Soc*. 2020;142:4298-4308.
176. Li Z, Zhang Q, Hencz L, et al. Multifunctional cation-vacancy-rich  $\text{ZnCo}_2\text{O}_4$  polysulfide-blocking layer for ultrahigh-loading Li-S battery. *Nano Energy*. 2021;89:106331.



177. Tian Y, Li G, Zhang Y, et al. Low-bandgap Se-deficient antimony selenide as a multifunctional polysulfide barrier toward high-performance lithium-sulfur batteries. *Adv Mater*. 2020;32:1904876.
178. Kong L, Chen X, Li BQ, et al. A bifunctional perovskite promoter for polysulfide regulation toward stable lithium-sulfur batteries. *Adv Mater*. 2018;30:1705219.
179. Luo D, Li G, Deng YP, et al. Synergistic engineering of defects and architecture in binary metal chalcogenide toward fast and reliable lithium-sulfur batteries. *Adv Energy Mater*. 2019;9:1900228.
180. Sun R, Bai Y, Bai Z, et al. Phosphorus vacancies as effective polysulfide promoter for high-energy-density lithium-sulfur batteries. *Adv Energy Mater*. 2022;12:2102739.
181. Zhang Z, Luo D, Li G, et al. Tantalum-based electrocatalyst for polysulfide catalysis and retention for high-performance lithium-sulfur batteries. *Matter*. 2020;3:920-934.
182. Liu F, Wang N, Shi C, et al. Phosphorus doping of 3D structural MoS<sub>2</sub> to promote catalytic activity for lithium-sulfur batteries. *Chem Eng J*. 2022;431:133923.
183. Zhang R, Dong Y, Al-Tahan MA, et al. Insights into the sandwich-like ultrathin Ni-doped MoS<sub>2</sub>/rGO hybrid as effective sulfur hosts with excellent adsorption and electrocatalysis effects for lithium-sulfur batteries. *J Energy Chem*. 2021;60:85-94.
184. Gao X, Yang X, Li M, et al. Cobalt-doped SnS<sub>2</sub> with dual active centers of synergistic absorption-catalysis effect for high-S loading Li-S batteries. *Adv Funct Mater*. 2019;29:1806724.
185. Li M, Yang D, Biendicho JJ, et al. Enhanced polysulfide conversion with highly conductive and electrocatalytic iodine-doped bismuth selenide nanosheets in lithium-sulfur batteries. *Adv Funct Mater*. 2022;32:2200529.
186. Wang M, Fan L, Sun X, et al. Nitrogen-doped CoSe<sub>2</sub> as a bifunctional catalyst for high areal capacity and lean electrolyte of Li-S battery. *ACS Energy Lett*. 2020;5:3041-3050.
187. Angamuthu G, Bosubabu D, Ramesha K, Rengarajan V. The Si<sub>3</sub>N<sub>4</sub>/MoS<sub>2</sub> hetero-structure as an effective polysulfide regulator for high-performance lithium-sulfur battery. *Appl Mater Today*. 2021;22:100916.
188. Ye C, Jiao Y, Jin H, et al. 2D MoN-VN heterostructure to regulate polysulfides for highly efficient lithium-sulfur batteries. *Angew Chem Int Ed*. 2018;57:16703-16707.
189. Lin H, Yang L, Jiang X, et al. Electrocatalysis of polysulfide conversion by sulfur-deficient MoS<sub>2</sub> nanoflakes for lithium-sulfur batteries. *Energy Environ Sci*. 2017;10:1476.
190. Yang C, Gong N, Chen T, et al. Enhanced catalytic conversion of polysulfides using high-percentage 1T-phase metallic WS<sub>2</sub> nanosheets for Li-S batteries. *Green Energy Environ*. 2022;7:1340.
191. Zha C, Yang F, Zhang J, Zhang T, Dong S, Chen H. Promoting polysulfide redox reactions and improving electronic conductivity in lithium-sulfur batteries via hierarchical cathode materials of graphene-wrapped porous TiO<sub>2</sub> microspheres with exposed (001) facets. *J Mater Chem A*. 2018;6:16574-16582.

## AUTHOR BIOGRAPHY



**Zijian Zheng** is a full professor at the Institute of Textiles and Clothing at The Hong Kong Polytechnic University. He received his BEng (2003) in chemical engineering at Tsinghua University, PhD (2007) in chemistry at the University of Cambridge, and postdoc training at Northwestern University (2008–2009). His research interests include surface and polymer science, nanofabrication, flexible and wearable materials, devices, and energy.

**How to cite this article:** Fan H, Luo W, Dou S, Zheng Z. Advanced two-dimensional materials toward polysulfides regulation of metal-sulfur batteries. *SmartMat*. 2023;4:e1186.  
doi:10.1002/smm2.1186